LETTER

doi:10.1038/nature14424

Allogeneic IgG combined with dendritic cell stimuli induce antitumour T-cell immunity

Yaron Carmi[1], Matthew H. Spitzer[1,2], Ian L. Linde[1], Bryan M. Burt[3], Tyler R. Prestwood[1], Nicola Perlman[1], Matthew G. Davidson[1], Justin A. Kenkel[1], Ehud Segal[1], Ganesh V. Pusapati[4], Nupur Bhattacharya[1] & Edgar G. Engleman[1]

Whereas cancers grow within host tissues and evade host immunity through immune-editing and immunosuppression[1–5], tumours are rarely transmissible between individuals. Much like transplanted allogeneic organs, allogeneic tumours are reliably rejected by host T cells, even when the tumour and host share the same major histocompatibility complex alleles, the most potent determinants of transplant rejection[6–10]. How such tumour-eradicating immunity is initiated remains unknown, although elucidating this process could provide the basis for inducing similar responses against naturally arising tumours. Here we find that allogeneic tumour rejection is initiated in mice by naturally occurring tumour-binding IgG antibodies, which enable dendritic cells (DCs) to internalize tumour antigens and subsequently activate tumour-reactive T cells. We exploited this mechanism to treat autologous and autochthonous tumours successfully. Either systemic administration of DCs loaded with allogeneic-IgG-coated tumour cells or intratumoral injection of allogeneic IgG in combination with DC stimuli induced potent T-cell-mediated antitumour immune responses, resulting in tumour eradication in mouse models of melanoma, pancreas, lung and breast cancer. Moreover, this strategy led to eradication of distant tumours and metastases, as well as the injected primary tumours. To assess the clinical relevance of these findings, we studied antibodies and cells from patients with lung cancer. T cells from these patients responded vigorously to autologous tumour antigens after culture with allogeneic-IgG-loaded DCs, recapitulating our findings in mice. These results reveal that tumour-binding allogeneic IgG can induce powerful antitumour immunity that can be exploited for cancer immunotherapy.

To study the basis of allogeneic tumour rejection, we examined the immune response to tumours in major histocompatibility complex (MHC)-matched allogeneic mice (illustrated in Fig. 1a). B16 melanoma cells expanded continuously in syngeneic C57BL/6 hosts yet spontaneously regressed in allogeneic 129S1 hosts (Fig. 1b). Conversely, liver-metastatic pancreatic tumour cells (LMP), isolated from $Kras^{G12D/+}$;LSL-$Trp53^{R172H/+}$;Pdx1-Cre mice[11], grew steadily in 129S1 mice but spontaneously regressed in C57BL/6 animals (Fig. 1b). Depletion of natural killer (NK) cells did not prevent tumour rejection (Extended Data Fig. 1a). In contrast, depletion of $CD4^+$ or $CD8^+$ T cells before allogeneic tumour inoculation prevented tumour regression (Fig. 1b). T-cell proliferation and tumour infiltration began by week 1 (Fig. 1c and Extended Data Fig. 1b). Additionally, allogeneic tumours contained more mature myeloid DCs (mDCs, $Ly6C^-CD11b^+CD11c^+MHCII^+CD64^{dim}$) and fewer $SSC^{low}CD11b^{hi}Ly6C^{hi}MHCII^-$ myeloid cells than syngeneic tumours (Fig. 1d and Extended Data Fig. 1c). Even at day 3, mDCs in allogeneic tumours expressed higher levels of MHCII, CD86 and CD40 compared to mDCs in syngeneic tumours, reflecting activation (Extended Data Fig. 1d). Allogeneic mDCs internalized more tumour-cell-derived molecules from CFSE-labelled LMP cells than syngeneic mDCs (Fig. 1e). However, co-culture of DCs with allogeneic tumour cells induced negligible activation or tumour antigen uptake (Fig. 1f and Extended Data Fig. 1e), demonstrating that additional factors contribute to DC activation *in vivo*.

Notably, IgM and IgG antibodies were bound to allogeneic, but not syngeneic, tumour cells within 24 h after tumour inoculation (Fig. 1g–i), before T cells appeared (Fig. 1c). Moreover, allogeneic antibodies bound tumour cells more effectively than syngeneic antibodies (Extended Data Fig. 2a), including syngeneic antibodies from tumour-bearing mice (Extended Data Fig. 2b). To assess the potential role of antibodies in tumour rejection, B cells were depleted before mice were challenged with allogeneic tumours (Extended Data Fig. 2c). Antibody depletion accelerated tumour development and delayed or prevented tumour rejection (Fig. 1j). Moreover, adoptive transfer of allogeneic IgG, but not IgM, enabled rejection of syngeneic tumours (Fig. 1k and Extended Data Fig. 2d). This effect was abrogated in Fcγ receptor (FcγR)-deficient mice (Fig. 1k).

To investigate the effect of antibodies on tumour uptake by DCs, we incubated tumour cells or lysates with syngeneic or allogeneic antibodies to form immune complexes and added these to bone-marrow-derived DCs (BMDCs) (Fig. 2a). Only immune complexes from allogeneic IgG (alloIgG-IC) or IgM (alloIgM-IC) induced BMDC activation and uptake of tumour-derived proteins (Fig. 2b–d), which were found in proximity to MHCII molecules (Fig. 2e). BMDCs activated by alloIgG-IC induced significant T-cell proliferation (Fig. 2f), demonstrating that tumour antigens were processed and presented.

To determine whether immune-complex-bound DCs could elicit antitumour immune responses in syngeneic hosts, B16 or LMP cells were inoculated subcutaneously, and tumours were removed upon reaching 25–55 mm^2, leaving tumour-free margins. IgG-IC or IgM-IC were prepared from excised tumours and incubated with syngeneic BMDCs, which were injected into the corresponding tumour-resected mouse (Fig. 2g). While nearly all mice treated with syngeneic BMDCs loaded with alloIgG-IC remained tumour-free for over a year, all other animals experienced rapid tumour relapse (Fig. 2h). This response was completely abrogated in DCs lacking FcγR (Extended Data Fig. 3a–c). Furthermore, adoptive transfer of T cells from alloIgG-IC-treated animals protected naive mice from tumour challenge (Extended Data Fig. 3d, e).

Despite these findings, only minor effects were observed when allogeneic IgG was injected into tumours in autologous hosts (Fig. 3a). To address this discrepancy, we obtained tumour-associated DCs (TADCs) (Extended Data Fig. 4a) and cultured them with tumour lysates or alloIgG-IC. In contrast to BMDCs, TADCs displayed no activation (Fig. 3b–d and Extended Data Fig. 4b) and their transfer to tumour-resected mice had no effect on recurrence (Fig. 3e). Accordingly, p38, ERK1/2 and JNK were phosphorylated in BMDCs but not TADCs activated with alloIgG-IC (Fig. 3f). We then tested the effect of additional MAPK stimuli on the response of TADCs to

[1]School of Medicine, Department of Pathology, Stanford University, Palo Alto, California 94305, USA. [2]School of Medicine, Baxter Laboratory in Stem Cell Biology, Department of Microbiology and Immunology, Stanford University, Palo Alto, California 94305, USA. [3]School of Medicine, Department of Cardiothoracic Surgery, Stanford University, Palo Alto, California 94305, USA. [4]School of Medicine, Department of Biochemistry, Stanford University, Palo Alto, California 94305, USA.

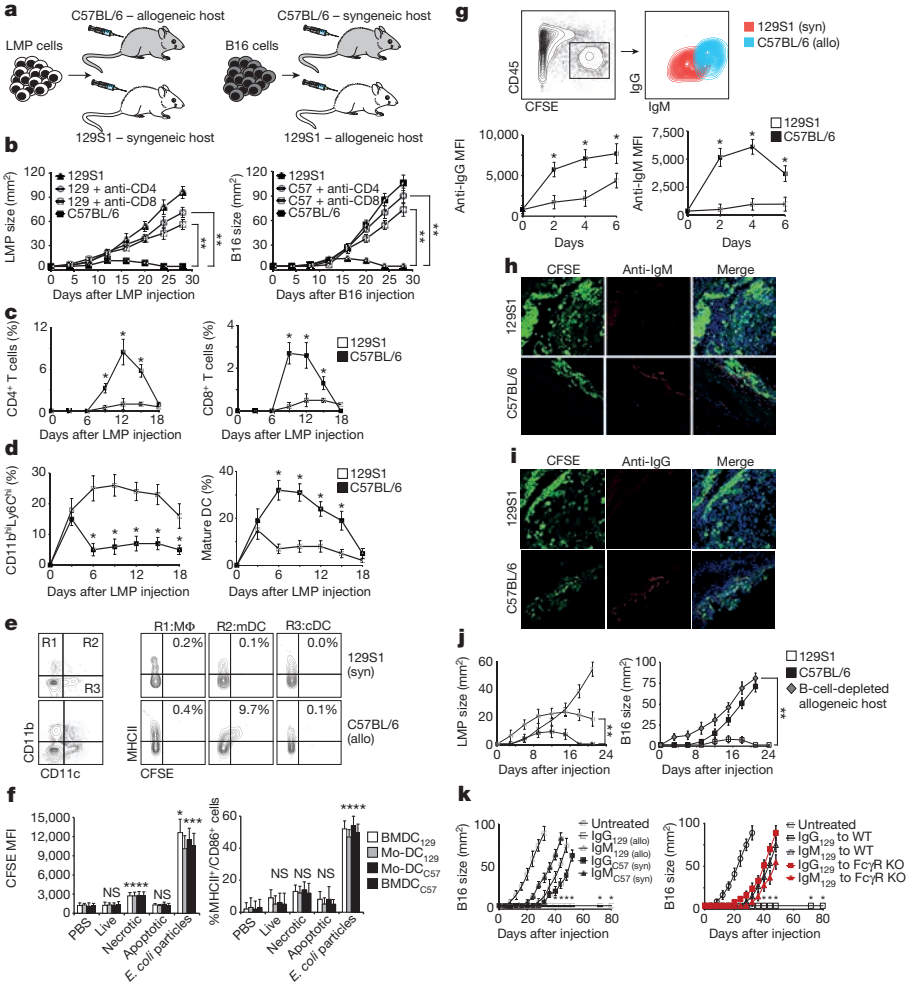

Figure 1 | Tumour-binding antibodies initiate rejection of allogeneic tumours. **a**, Experimental design: injection of LMP and B16 cells subcutaneously into syngeneic and allogeneic hosts. **b**, Growth of LMP and B16 tumours in C57BL/6, 129S1, $CD4^+$ cell-depleted or $CD8^+$ cell-depleted allogeneic mice ($n = 6$, 3 independent experiments). **c**, Percentages of LMP-infiltrating $CD4^+$ and $CD8^+$ T cells among $CD45^+$ cells ($n = 5$, 3 independent experiments). **d**, Percentages of LMP-infiltrating $CD11b^{hi}Ly6C^{hi}$ cells and mature DCs among total cells ($n = 4$, 3 independent experiments). **e**, Myeloid cells in the draining lymph nodes of mice inoculated with CFSE-labelled LMP cells 3 days earlier ($n = 5$, 3 independent experiments). R1, macrophages; R2, myeloid dendritic cells; R3, classical dendritic cells. **f**, Tumour uptake, MHCII and CD86 expression by BMDCs and blood monocyte-derived (Mo) DCs incubated overnight with CFSE-labelled live, frozen/thawed (necrotic), or mitomycin-C-treated (apoptotic) LMP cells or fluorescein-labelled *Escherichia coli* BioParticles ($n = 4$, 4 independent experiments). MFI, mean fluorescence intensity. **g**, IgG and IgM bound *in vivo* to CFSE-labelled LMP cells 48 h after tumour inoculation ($n = 5$, 4 independent experiments). **h**, **i**, Representative staining of tumour sections by IgM and IgG 24 h after inoculation of CFSE-labelled LMP cells. Original magnification, 200×; 3 independent experiments. **j**, Tumour size in 129S1, C57BL/6 and B-cell-depleted allogeneic hosts ($n = 5$, 3 independent experiments). **k**, B16 size in naive mice or mice injected with syngeneic or allogeneic antibodies ($n = 5$). B16 size in naive C57BL/6 and FcγR knockout (KO) mice injected with allogeneic antibodies ($n = 5$, 3 independent experiments). Experiments were independently repeated at least 3 times and analysed by Mann–Whitney *U* test. $*P < 0.05$; $**P < 0.01$; NS, not significant. Error bars represent s.e.m. unless specified otherwise.

alloIgG-IC. Poly(I:C), TNFα + CD40L or IFNγ + CD40L enabled activation of TADCs and alloIgG-IC uptake (Fig. 3g and Extended Data Fig. 4c, d). We subsequently tested whether allogeneic IgG in combination with one of these stimuli could induce immune responses to syngeneic tumours *in situ*. Intratumoral injection of allogeneic IgG combined with TNFα + CD40L or poly(I:C) induced complete elimination of B16 and LL/2 tumours (Fig. 4a and Extended Data Fig. 5a–c).

Under these conditions, only mDCs ($CD11b^+Ly6C^-CD11c^+MHCII^+CD64^{dim}$) and cDCs ($CD11b^-CD11c^{hi}MHCII^+$) markedly increased their IgG binding during an effective antitumour immune response (Fig. 4b and Extended Data Fig. 5d). Moreover, tumour-infiltrating DCs exhibited significant activation (Fig. 4c) and accumulation in the draining lymph nodes (Extended Data Fig. 5e). Adoptive transfer of TADCs from treated mice into naive mice conferred complete protection against B16 (Fig. 4d). In contrast, transfer of macrophages had a modest protective effect, while B cells, NK cells and mast cells provided no benefit (Extended Data Fig. 5f, g).

To test whether allogeneic IgG bears unique modifications that mediate an immune response, we covalently crosslinked syngeneic IgG onto B16 membrane proteins. These immune complexes still conferred a therapeutic benefit after incubation with BMDCs (Extended Data Fig. 6a), demonstrating that binding of IgG to the tumour cell surface, rather than the origin of the IgG, was critical. To investigate whether the tumour-binding antibody targets are related to the antitumour T-cell specificities, we resected B16 tumour cells and formed immune complexes using an antibody against MHC-I, against which there could not be reactive T cells. DCs loaded with these immune complexes protected mice from B16 recurrence without inducing autoimmunity, suggesting that tumour-reactive T-cell specificity is not determined by the antibody targets (Extended Data Fig. 6b). Furthermore, B16-bearing mice treated with allogeneic IgG + anti-CD40 + TNFα were protected from re-challenge with B16 melanoma, but not syngeneic RMA lymphoma, suggesting that the tumour-reactive T cells recognize

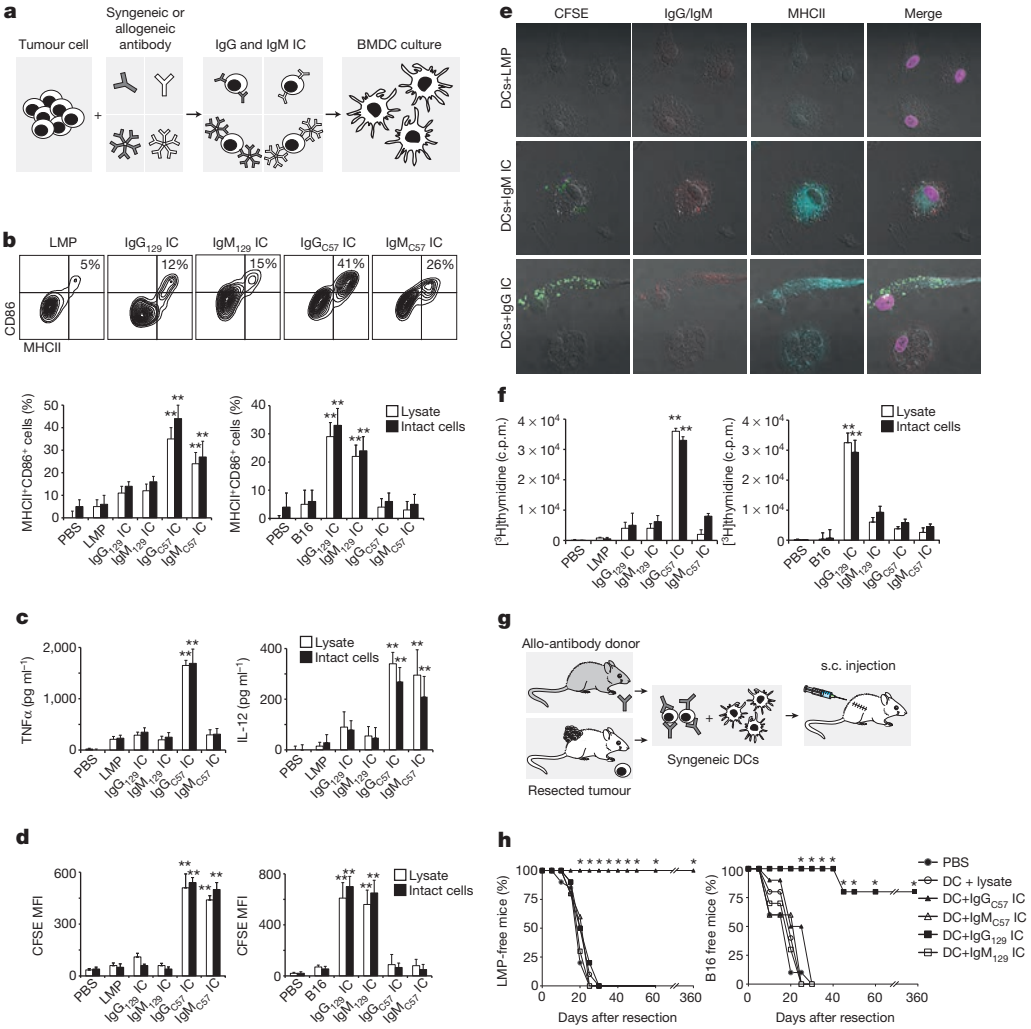

Figure 2 | AlloIgG-IC are internalized and presented by BMDCs and drive protective immunity *in vivo*. **a**, Experimental design: tumour cells or lysates were incubated with syngeneic or allogeneic antibodies and then cultured with BMDCs overnight. **b**, Expression of CD86 and MHCII on BMDCs cultured with antibody-coated tumour lysates or intact tumour cells ($n = 5, 10$ independent experiments). IC, immune complexes. **c**, TNFα and IL-12 in supernatants of BMDCs cultured overnight with immunoglobulin immune complexes formed with LMP lysate or intact LMP cells ($n = 5, 4$ independent experiments). **d**, Internalization of CFSE in BMDCs incubated overnight with immunoglobulin immune complexes formed from CFSE-labelled tumour lysates or CFSE-labelled intact cells ($n = 4, 10$ independent experiments). **e**, Representative localization of MHCII and immunoglobulin immune complexes on BMDCs cultured overnight with CFSE-labelled LMP cells coated with allogeneic antibodies (original magnification, 400×; 3 independent experiments). **f**, Proliferation of $CD4^+$ T cells cultured with DCs loaded with immune complexes formed from LMP and B16 lysates or intact cells ($n = 5, 5$ independent experiments). c.p.m., counts per minute. **g**, Experimental design: tumours were removed from mice, coated with antibodies, incubated for 24 h with BMDCs, and injected subcutaneously into corresponding tumour-resected mice. **h**, Tumour recurrence in mice treated with BMDCs loaded with tumour lysate incubated with allogeneic or syngeneic antibodies ($n = 5, 3$ independent experiments). Experiments were independently repeated at least 3 times and analysed by Mann–Whitney *U* test. $*P < 0.05$; $**P < 0.01$. Error bars represent s.e.m. unless specified otherwise.

tumour-associated antigens rather than widely expressed allo-antigens (Extended Data Fig. 6c).

Vaccination with BMDCs loaded with immune complexes containing B16 proteins derived from the cell membrane, but not other subcellular fractions, prevented tumour relapse, and B16 protein denaturation, but not deglycosylation, removed the therapeutic benefit (Extended Data Fig. 6d). Pre-absorbing allogeneic IgG against normal cells syngeneic to the tumour also removed the therapeutic benefit (Extended Data Fig. 6e). Allogeneic IgG from germ-free mice induced tumour immunity (Extended Data Fig. 6f), suggesting that IgG against microbiota was not required. Therefore, the protective effect of allogeneic IgG is dependent on antibody binding to membrane proteins expressed on normal cells.

We therefore identified B16 membrane proteins specifically bound by allogeneic IgG using mass spectrometry. While syngeneic IgG bound six cell membrane proteins, all at approximately equal or lower levels than allogeneic IgG, allogeneic IgG preferentially bound sixteen cell membrane proteins, many containing strain-specific polymorphisms (Extended Data Table 1). To validate these hits functionally, we focused on transmembrane-glycoprotein NMB (GPNMB). Antibodies against GPNMB bound B16 cells at much higher levels than normal cells and enabled DC activation, and allogeneic IgG bound GPNMB at higher levels than syngeneic IgG (Extended Data Fig. 7a–c). Treatment using anti-GPNMB + anti-CD40 + TNFα induced significant FcγR-dependent tumour regression (Extended Data Fig. 7d, e). Treated tumours exhibited marked leukocyte infiltration, including activated effector/memory T cells, compared to untreated tumours (Extended Data Fig. 8a, b). Whereas all treatments elicited gp100-reactive $CD8^+$ T cells, only allogeneic IgG + antiCD40 + TNFα elicited Trp2-reactive $CD8^+$ T cells (Extended Data Fig. 8c). Adoptive transfer of CD4 or CD8 T cells from these mice protected naive mice from B16 challenge, and depletion of either CD4 or CD8 T cells before treatment prevented

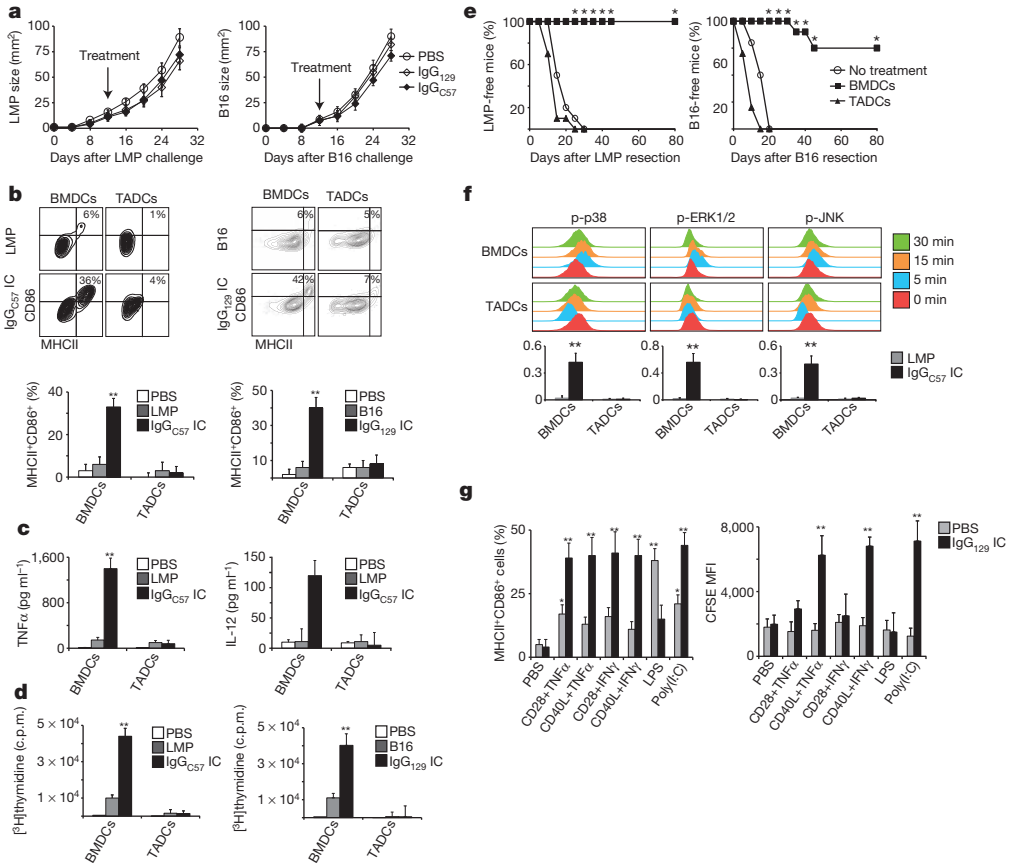

Figure 3 | TADCs, but not BMDCs, require stimulation to respond to alloIgG-IC. **a**, Tumour growth following intratumoral injection of PBS, 129S1 IgG or C57BL/6 IgG ($n = 6$, 3 independent experiments). **b**, CD86 and MHCII expression on DCs incubated with PBS, tumour lysates or alloIgG-IC ($n = 5$, 10 independent experiments). **c**, TNFα and IL-12 in the supernatants of DCs cultured with PBS control, LMP lysate or alloIgG-IC ($n = 5$, 4 independent experiments). **d**, Proliferation of $CD4^+$ T cells cultured with DCs treated with PBS, tumour lysate, or alloIgG-IC ($n = 5$, 5 independent experiments). **e**, Recurrence of resected LMP and B16 in untreated mice or mice treated with alloIgG-IC-activated BMDCs or TADCs ($n = 5$, 3 independent experiments). **f**, Phosphorylated (p)-p38, pERK1/2 and pJNK levels in DCs, untreated or incubated with alloIgG-IC. Graphs show arcsinh ratios of phospho-species in DCs incubated for 5 min with LMP lysate or alloIgG-IC over baseline levels from unstimulated DCs ($n = 5$, 5 independent experiments). **g**, MHCII and CD86 expression and CFSE internalization by TADCs after overnight culture with CFSE-labelled alloIgG-IC ($n = 4$, 10 independent experiments). Experiments were independently repeated at least 3 times and analysed by Mann–Whitney *U* test. $*P < 0.05$; $**P < 0.01$. Error bars represent s.e.m. unless specified otherwise.

tumour regression (Extended Data Fig. 8d, e). These findings confirm that allogeneic IgG induces T-cell reactivity against tumour-associated antigens distinct from those bound by the antibodies.

We next treated a genetically engineered melanoma model driven by $Braf^{V600E}$ and loss of *Pten* (ref. 12) with allogeneic IgG + anti-CD40 + TNFα. Treated mice experienced complete responses lasting over 8 weeks in the injected tumours and distant sites (Fig. 4e). To assess the effect of this combination on metastases, orthotopic 4T1 breast tumours were treated after all mice had palpable tumour-draining lymph nodes, indicative of tumour spread. Only treatment with allogeneic IgG + anti-CD40 + TNFα led to almost complete resolution of metastases and primary tumours, and the few remaining micrometastases were heavily infiltrated with leukocytes (Fig. 4f, g and Extended Data Fig. 9a).

We next compared the capacity of IgG from cancer patients and healthy allogeneic donors to bind the patients' tumours. Most but not all donors had antibodies with higher tumour-binding capacity (Extended Data Fig. 9b). We tested whether allogeneic IgG + CD40L + TNFα could induce tumour uptake and maturation of human TADCs from two patients with lung carcinoma. Addition of CD40L + TNFα enabled these DCs to internalize alloIgG-IC and induced DC activation (Fig. 4h and Extended Data Fig. 9c, d). Moreover, BMDCs from two patients with malignant pleural mesothelioma incubated with alloIgG-IC, but not autologous IgG-IC, exhibited activation and drove autologous $CD4^+$ T-cell proliferation (Fig. 4i).

The effect of naturally arising tumour-reactive antibodies on tumour progression has been a source of controversy. Some studies suggest that such antibodies promote tumour progression[13–19], while others report that they can stimulate antitumour immunity[20–28]. Like the antibodies that develop in cancer patients, commercial immunoglobulin preparations, which probably contain tumour-binding alloantibodies, have shown limited benefit when used to treat cancer[29,30]. Our data may provide a mechanistic explanation for these findings, as they show that while TADCs are not naturally responsive to IgG-IC, addition of specific stimuli enables them to drive tumour-eradicating immunity. Hence, the role that tumour-binding antibodies have in tumour immunity depends upon the environmental context and the cell types involved.

Here we demonstrate that tumour-antigen presentation after antibody-mediated uptake by DCs is sufficient to initiate protective T-cell-mediated immunity against tumours. Our work suggests that this fundamental mechanism of immunological recognition and targeting, which prevents tumour transmission even between MHC-matched individuals, can be exploited as a powerful therapeutic strategy for cancer.

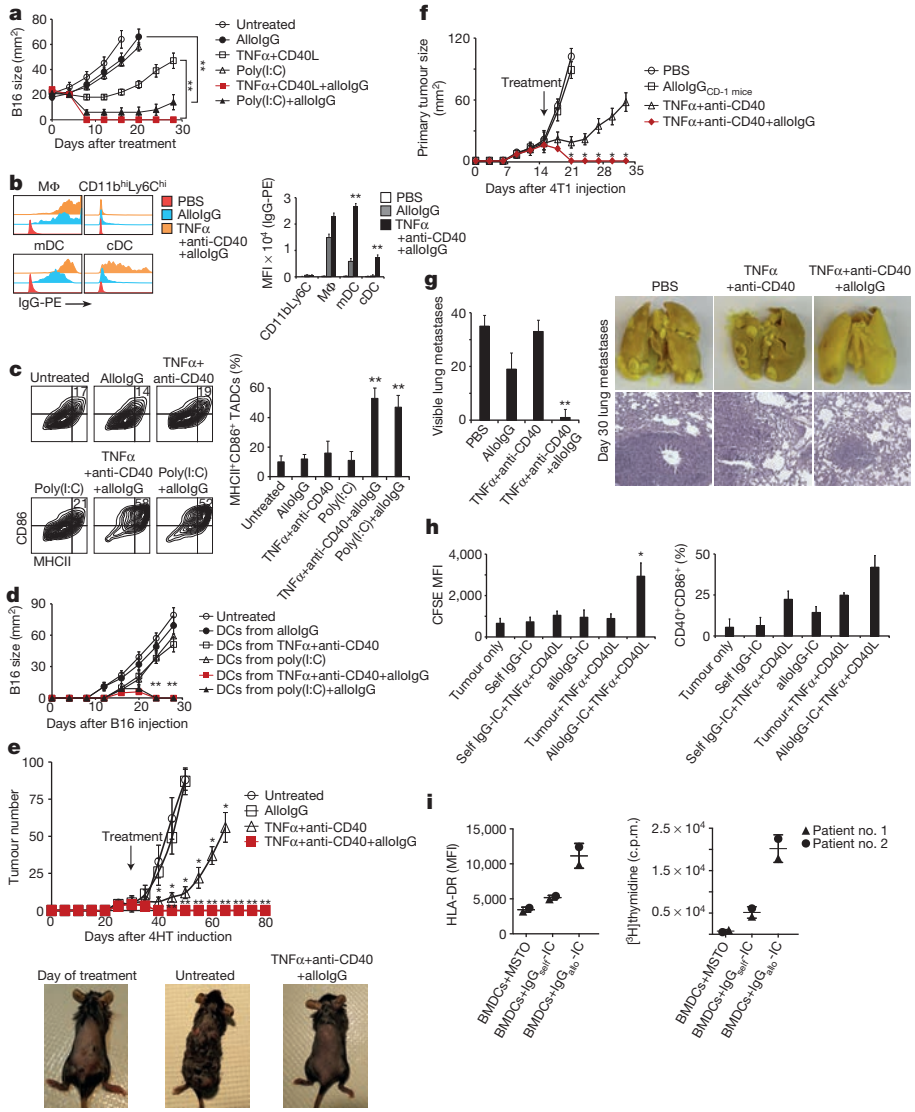

Figure 4 | Injection of tumours *in situ* with alloantibodies in combination with CD40 agonists and TNFα induces systemic DC-mediated antitumour immunity. **a**, Growth of tumours injected with allogeneic IgG (alloIgG), with or without immune stimuli ($n = 6$, 3 independent experiments). **b**, Mean fluorescence of phycoerythrin in myeloid cells from B16-bearing mice 2 h after treatment ($n = 4$, 3 independent experiments). **c**, CD86 and MHCII expression on DCs from B16 tumours 5 days after treatment ($n = 6$, 3 independent experiments). **d**, B16 growth in mice vaccinated with 2×10^6 DCs transferred from treated or untreated B16 tumours ($n = 6$, 3 independent experiments). **e**, Tumour number in Tyr:CreER;Braf^{V600E}/Pten$^{lox/lox}$ mice following treatment ($n = 4$, 3 independent experiments). Photographs show representative mice on the day of treatment and after day 24. **f**, 4T1 tumour size in mice following treatment ($n = 5$, 3 independent experiments). **g**, Mean counts of visible lung metastases, photographs and histology on day 30 (original magnification, 10×; $n = 5$, 3 independent experiments). **h**, CFSE internalization and CD40/CD86 co-expression on TADCs from lung cancer patients cultured overnight with CFSE-stained autologous tumour cells coated with self IgG or alloIgG ($n = 2$). **i**, HLA-DR upregulation by DCs (left) and proliferative response of CD4$^+$ T cells (right) from mesothelioma (MSTO) patients after culture of autologous BMDCs with self IgG- or alloIgG-coated autologous tumour cells ($n = 2$). Mouse experiments were independently repeated at least 3 times and analysed by Mann–Whitney *U* test.

Online Content Methods, along with any additional Extended Data display items and Source Data, are available in the online version of the paper; references unique to these sections appear only in the online paper.

Received 7 May 2014; accepted 24 March 2015.
Published online 29 April 2015.

1. Coussens, L. M., Zitvogel, L. & Palucka, A. K. Neutralizing tumor-promoting chronic inflammation: a magic bullet? *Science* **339,** 286–291 (2013).
2. Grivennikov, S. I., Greten, F. R. & Karin, M. Immunity, inflammation, and cancer. *Cell* **140,** 883–899 (2010).
3. Hanahan, D. & Coussens, L. M. Accessories to the crime: functions of cells recruited to the tumor microenvironment. *Cancer Cell* **21,** 309–322 (2012).
4. Schreiber, R. D., Old, L. J. & Smyth, M. J. Cancer immunoediting: integrating immunity's roles in cancer suppression and promotion. *Science* **331,** 1565–1570 (2011).
5. Vesely, M. D., Kershaw, M. H., Schreiber, R. D. & Smyth, M. J. Natural innate and adaptive immunity to cancer. *Annu. Rev. Immunol.* **29,** 235–271 (2011).
6. Manning, T. C. *et al.* Antigen recognition and allogeneic tumor rejection in CD8$^+$ TCR transgenic/RAG$^{-/-}$ mice. *J. Immunol.* **159,** 4665–4675 (1997).
7. Ferrara, J., Guillen, F. J., Sleckman, B., Burakoff, S. J. & Murphy, G. F. Cutaneous acute graft-versus-host disease to minor histocompatibility antigens in a murine model: histologic analysis and correlation to clinical disease. *J. Invest. Dermatol.* **86,** 371–375 (1986).
8. Appelbaum, F. R. Haematopoietic cell transplantation as immunotherapy. *Nature* **411,** 385–389 (2001).
9. Bishop, M. R. *et al.* Allogeneic lymphocytes induce tumor regression of advanced metastatic breast cancer. *J. Clin. Oncol.* **22,** 3886–3892 (2004).
10. Goulmy, E. Minor histocompatibility antigens: allo target molecules for tumor-specific immunotherapy. *Cancer J.* **10,** 1–7 (2004).
11. Tseng, W. W. *et al.* Development of an orthotopic model of invasive pancreatic cancer in an immunocompetent murine host. *Clin. Cancer Res.* **16,** 3684–3695 (2010).
12. Dankort, D. *et al.* *Braf*^{V600E} cooperates with *Pten* loss to induce metastatic melanoma. *Nature Genet.* **41,** 544–552 (2009).
13. Qin, Z. *et al.* B cells inhibit induction of T cell-dependent tumor immunity. *Nature Med.* **4,** 627–630 (1998).

14. de Visser, K. E., Korets, L. V. & Coussens, L. M. *De novo* carcinogenesis promoted by chronic inflammation is B lymphocyte dependent. *Cancer Cell* **7,** 411–423 (2005).
15. Andreu, P. *et al.* FcRγ activation regulates inflammation-associated squamous carcinogenesis. *Cancer Cell* **17,** 121–134 (2010).
16. Gerber, J. S. & Mosser, D. M. Reversing lipopolysaccharide toxicity by ligating the macrophage Fcγ receptors. *J. Immunol.* **166,** 6861–6868 (2001).
17. Willimsky, G. *et al.* Immunogenicity of premalignant lesions is the primary cause of general cytotoxic T lymphocyte unresponsiveness. *J. Exp. Med.* **205,** 1687–1700 (2008).
18. Soussi, T. p53 Antibodies in the sera of patients with various types of cancer: a review. *Cancer Res.* **60,** 1777–1788 (2000).
19. Gumus, E. *et al.* Association of positive serum anti-p53 antibodies with poor prognosis in bladder cancer patients. *Int. J. Urol.* **11,** 1070–1077 (2004).
20. Li, Q. *et al.* Adoptive transfer of tumor reactive B cells confers host T-cell immunity and tumor regression. *Clin. Cancer Res.* **17,** 4987–4995 (2011).
21. DiLillo, D. J., Yanaba, K. & Tedder, T. F. B cells are required for optimal $CD4^+$ and $CD8^+$ T cell tumor immunity: therapeutic B cell depletion enhances B16 melanoma growth in mice. *J. Immunol.* **184,** 4006–4016 (2010).
22. Clynes, R., Takechi, Y., Moroi, Y., Houghton, A. & Ravetch, J. V. Fc receptors are required in passive and active immunity to melanoma. *Proc. Natl Acad. Sci. USA* **95,** 652–656 (1998).
23. Nimmerjahn, F. & Ravetch, J. V. Divergent immunoglobulin g subclass activity through selective Fc receptor binding. *Science* **310,** 1510–1512 (2005).
24. Hamanaka, Y. *et al.* Circulating anti-MUC1 IgG antibodies as a favorable prognostic factor for pancreatic cancer. *Int. J. Cancer* **103,** 97–100 (2003).
25. Kurtenkov, O. *et al.* Humoral immune response to MUC1 and to the Thomsen-Friedenreich (TF) glycotope in patients with gastric cancer: relation to survival. *Acta Oncol.* **46,** 316–323 (2007).
26. Schuurhuis, D. H. *et al.* Immune complex-loaded dendritic cells are superior to soluble immune complexes as antitumor vaccine. *J. Immunol.* **176,** 4573–4580 (2006).
27. Regnault, A. *et al.* Fcγ receptor-mediated induction of dendritic cell maturation and major histocompatibility complex class I-restricted antigen presentation after immune complex internalization. *J. Exp. Med.* **189,** 371–380 (1999).
28. Rafiq, K., Bergtold, A. & Clynes, R. Immune complex-mediated antigen presentation induces tumor immunity. *J. Clin. Invest.* **110,** 71–79 (2002).
29. Schachter, J. *et al.* Efficacy and safety of intravenous immunoglobulin in patients with metastatic melanoma. *Ann. NY Acad. Sci.* **1110,** 305–314 (2007).
30. Fishman, P., Bar-Yehuda, S. & Shoenfeld, Y. IVIg to prevent tumor metastases. *Int. J. Oncol.* **21,** 875–880 (2002).

Acknowledgements We thank F. C. Grumet and N. E. Reticker-Flynn for helpful discussion. We also thank J. Sonnenburg for providing gnotobiotic mice. This work was supported by NIH grants U01 CA141468 and 5T32AI007290-27. M.H.S. is supported by NIH NRSA F31CA189331. I.L.L. is supported by a Smith Stanford Graduate Fellowship.

Author Contributions Y.C. conceived the study, performed experiments and wrote the manuscript. M.H.S., I.L.L., T.R.P. and N.B. performed experiments, helped with experimental design and contributed to manuscript preparation. B.M.B. helped with experimental design, human tissue acquisition and manuscript preparation. N.P., M.G.D., J.A.K., E.S. and G.V.P. performed experiments. E.G.E. supervised the project, analysed data and wrote the manuscript.

Author Information Reprints and permissions information is available at www.nature.com/reprints. The authors declare no competing financial interests. Readers are welcome to comment on the online version of the paper. Correspondence and requests for materials should be addressed to E.G.E. (edengleman@stanford.edu) or Y.C. (ycarmi76@stanford.edu).

METHODS

Mice. 129S1/SvlmJ mice, C57Bl/6 wild-type (WT) mice, Balb/c mice, and mice that develop inducible melanoma (B6.Cg-Braf^{tm1Mmcm}/Pten^{tm1Hwu}Tg (Tyr-cre/ERT2)13Bos/BosJ) were purchased from the Jackson Laboratory (Bar Harbour, Maine) and bred on-site. CD-1 outbred mice and *FcγR*$^{-/-}$ (B6.129P2-*Fcer1g*^{tm1Rav}) mice were purchased from Taconic (Germantown, NY). 12–16-week-old male and female mice were sorted randomly into groups before assigning treatment conditions. No blinded experiments were conducted. All mice were maintained in an American Association for the Accreditation of Laboratory Animal Care–accredited animal facility. All protocols were approved by the Stanford University Institutional Animal Care and Use Committee under protocol APLAC-17466.

Cell lines. The mouse lines B16F10 (melanoma), 4T-1.1 (breast cancer), LL/2 (Lewis lung carcinoma) and RMA (lymphoma) were all purchased from the ATCC. LMP pancreas tumour cells were isolated from Kras$^{G12D/+}$; LSL-Trp53$^{R172H/+}$; Pdx-1-Cre mice in our laboratory as described[11]. Cells were cultured in DMEM (Gibco, Carlsbad, California) supplemented with 10% heat-inactivated FCS, 2 mM L-glutamine, 100 U ml^{-1} penicillin and 100 μg ml^{-1} streptomycin (Gibco) under standard conditions. Cell lines were tested for mycoplasma contamination and endotoxin.

Preparation and *in vitro* studies of mouse DC subsets. Bone marrow mononuclear cells were negatively selected using a murine monocyte enrichment kit (Stem Cell Technologies, Vancouver, Canada), and FSC^{lo}SSC^{lo}Ly6C^{hi}CD115^{hi}MHCII^{-} cells were sorted with a FACS Aria II (BD Biosciences). Monocytes were cultured for 4–5 days in the presence of 50 ng ml^{-1} GM-CSF (PeproTech) to generate DCs. For TADCs, tumours were digested in Hank's balanced salt solution (HBSS, Gibco) containing 4 mg ml^{-1} collagenase IV and 0.01 mg ml^{-1} DNase I (Sigma). Cells were applied on a Ficoll gradient and magnetically enriched using CD11b^{+} selection kits (StemCells) and Ly6C^{-}CD11c^{+}MHCII^{+} cells were sorted by FACS. In some experiments TADCs were activated with 1 μg ml^{-1} bacterial lipopolysaccharide (LPS), 1 μg ml^{-1} high molecular mass polyinosinic-polycytidylic acid (poly(I:C)) (both from InvivoGen, San Diego, California), or with 50 ng ml^{-1} TNFα or 50 ng ml^{-1} IFNγ (PeproTech) in combination with 500 ng ml^{-1} CD40L, OX-40 (PeproTech) or 500 ng ml^{-1} CD28 (R&D) recombinant mouse proteins. All *in vitro* activations of mouse DCs were independently repeated at least 10 times in duplicate.

Preparation and *in vitro* studies of tumour cells, TADCs, autologous T cells and IgG from patients with cancer. Tumour cells, TADCs, peripheral blood T cells and IgG were obtained from two patients undergoing resection surgery for stage I lung carcinoma. Tumours were enzymatically digested with 0.1 mg ml^{-1} of DNase I and 5 mg ml^{-1} collagenase IV (Sigma) in HBSS for 30 min. Tumour cells were enriched by sorting CD45-negative cells, fixed in 2% paraformaldehyde for 20 min, washed extensively in PBS and coated for 30 min with autologous IgG or pooled allogeneic IgG obtained from healthy blood donors. To obtain TADCs, FSC^{low}SSC^{low}CD11c^{+}MHCII^{hi} cells were sorted and maintained for 1 h in 10% FCS IMDM at 37 °C. For FACS and confocal studies, tumour DCs were incubated overnight with autologous tumour cells coated with self IgG or alloIgG alone, or in the presence of 5 ng ml^{-1} recombinant human TNFα and 500 ng ml^{-1} CD40L (PeproTech).

In separate experiments, 10-cm-long rib bones and 10 ml blood were obtained from two patients undergoing resection surgery for malignant pleural mesothelioma. To generate BMDCs, bones were flushed with PBS and mononuclear cells were separated on Ficoll gradients. CD34^{+} cells were then enriched using magnetic beads (Miltenyi) and cultured for 9–12 days in IMDM (Gibco) supplemented with 10% FCS, 50 ng ml^{-1} human GM-CSF and 20 ng ml^{-1} human IL-4 (PeproTech). To obtain autologous tumour cells, tumours were enzymatically digested with 0.1 mg ml^{-1} of DNase I and 5 mg ml^{-1} collagenase IV (Sigma) in HBSS for 30 min. Tumour cells were enriched by sorting CD45-negative cells, fixed in 2% paraformaldehyde for 20 min, washed extensively in PBS and coated for 30 min with autologous or pooled allogeneic IgG. Autologous CD4^{+} T cells were enriched from peripheral blood mononuclear cells on magnetic beads (Miltenyi) and IgG was isolated from each patient's plasma using protein A columns (GE Healthcare). For T-cell proliferation assays, 2 × 10^{4} DCs were incubated overnight with antibody-coated tumour cells as above, washed and co-cultured with 2 × 10^{5} autologous CD4^{+}-enriched T cells. After 6 days, cells were pulsed with [^{3}H]thymidine (1 μCi per well) and cultured for an additional 18 h before being harvested in a Harvester 400 (Tomtec). Radioactivity was measured by a 1450 MicroBeta counter (LKB Wallac). T-cell proliferation was assayed in six technical replicates per sample. The human subject's protocols were approved by Stanford's Institutional Review Board, and informed consent was obtained from all subjects.

Flow cytometry. For cell surface staining, monoclonal antibodies conjugated to FITC, PE, PE-Cy7, PE-Cy5.5, APC-Cy7, eFluor 650, or Pacific blue and specific for the following antigens were used: CD11b (M1/70), F4/80 (BM8), B220 (RA3-6B2) from BioLegend (San Diego, California) and CD115 (AFS98), CD80 (16-10A1), I-Ab (AF6-120.1), CD40 (1C10), Ly6C (HK1.4), CD86 (GL1) from eBioscience (San Diego, California). All *in vivo* experiments to characterize tumour-infiltrating leukocytes were independently repeated at least three times with 3–5 mice per group. iTAg APC-labelled H-2K^{b}-Trp-2(SVYDFFVWL) and iTAg PE-labelled H-2D^{b}-gp100(EGSRNQDWL) tetramers were purchased from MBL international (Woburn, Massachusetts) and were used according to the manufacturer's instructions. Tetramer-staining experiments were repeated twice with five 5 mice in each group. For protein phosphorylation-specific flow cytometry, cells were activated for 5, 15 or 30 min with or without IC and fixed for 15 min with 1.8% paraformaldehyde. Cells were washed twice with PBS containing 2% FCS and incubated with 95% methanol at 4 °C for 20 min. Conjugated antibodies against phospho-p38 (Thr180/Tyr182) and phospho-JNK (Thr183/Tyr185) were purchased from Cell Signaling and phospho-ERK1/2 (p44) (pT202/pY204) from BD Biosciences. DC protein phosphorylation experiments were repeated five times, each with biological duplicates. For tumour-binding IgM and IgG, PE-conjugated anti-mouse IgM (RMM-1), anti-mouse IgG (Poli4052) and anti-human IgG (HP6017) were purchased from BioLegend. Flow cytometry was performed on a LSRII (BD Biosciences) and data sets were analysed using FlowJo software (Tree Star, Inc.). *In vivo* binding levels were tested in four independent experiments, 3–5 mice in each group.

Intracellular IFNγ staining. B16 tumours from treated mice were digested to obtain a single cell suspension. A total of 2 × 10^{6} cells per well were cultured for 4 h in 10% FCS RPMI containing 1× Brefeldin A (eBioscience) in a 96-well plate containing 4 × 10^{4} BMDCs loaded with 10 μg of B16 membrane proteins. Cells were washed and stained for extracellular T-cell markers. Cells were then fixed and permeabilized using cytofix/cytoperm solutions (BD Bioscience) and stained with PE-Cy7 conjugated anti-IFNγ antibody (XMG1.2, BioLegend). Experiments were repeated twice independently with 5 mice per group.

Cytokine measurements. Cells were seeded at 1 × 10^{6} cells ml^{-1} and cultured for 12 h with or without tumour immune complexes, or LPS (Sigma). TNFα, IFNγ and IL-12 (p40/p70) in the supernatants were measured by ELISA, according to manufacturer's instructions (R&D Systems, Minneapolis, Minnesota). Cytokine secretion was measured in biological triplicates in four independent experiments.

IgG and IgM purification and measurement. Mouse antibodies were obtained from pooled 5-ml 20–24-week-old mouse serum by liquid chromatography on AKTA Explorer/100Air (GE Healthcare). Total mouse IgG and IgM were purified using protein-G and 2-mercaptopyridine columns, respectively (GE Healthcare). The levels of purified IgG and IgM were measured with specific ELISA kits (Bethyl, Montgomery, Texas) according to manufacturer's instructions. The capacity of purified antibodies to bind tumour cells was tested by flow cytometry before their use *in vivo*. 1 μg IgG per 1 × 10^{5} allogeneic tumour cells bound at least 8 times higher compared to isotype control antibodies. Serum levels of antibodies were measured in biological triplicates in four independent experiments.

Necrotic and apoptotic tumour cell internalization experiments. For necrotic tumour cells, cultured LMP or B16 cells were trypsinized, washed and re-suspended at a concentration of 5 × 10^{6} cells ml^{-1} in cold PBS (GIBCO). Cells were then subjected to three cycles of freeze–thaw between liquid nitrogen and a 37 °C water bath and the level of necrotic cells was determined by Trypan blue under light microscopy. Apoptotic tumour cells were prepared by their pre-incubation with 25 μg ml^{-1} of mitomycin C (Sigma) for 1 h in antibiotic and serum-free DMEM. Fluorescein-labelled *E. coli* BioParticles were purchased from Life Technologies and used according to the manufacturer's instructions. Dendritic cell activations with above cells were repeated four independent times in biological duplicates.

Preparation of antibody–tumour lysate immune complexes and antibody-bound tumour cells. When obtained from surgical resections, tumour cells were initially isolated after enzymatic digestion and sorted as FSC^{hi}CD45^{-} cells before their fixation and staining. For tumour–antibody complexes, tumour cells were fixed in 2% paraformaldehyde, washed extensively and incubated with 1–3 μg syngeneic or allogeneic IgG or IgM per 1 × 10^{5} tumour cells, and were then washed to remove excess antibodies. To obtain tumour lysate immunoglobulin immune complexes, tumour cells were incubated for 30 min on ice with 1–3 μg syngeneic or allogeneic IgG or IgM per 1 × 10^{5} tumour cells, washed from excess antibodies and further disrupted with non-denaturing lysis buffer (Pierce) to obtain immunoglobulin immune complexes. Dendritic cell activations with the above immunoglobulin immune complexes were repeated in at least 10 independent experiments in biological duplicates.

Absorption of allogeneic IgG on normal cells. Skin and pancreas were removed from naive C57BL/6 or 129S1 mice and enzymatically digested with 0.1 mg ml^{-1} of DNase I (Sigma) and 4 mg ml^{-1} collagenase IV (Sigma) in PBS to obtain single cell suspensions. Splenocytes were isolated by mashing spleens through 70 μm cell strainers. Cells were then mixed at 1:1:1 ratio and extensively washed and

incubated with 0.5 μg per 1×10^6 cells FcγR block (BD) and 5% (W/V) BSA (Sigma) in PBS for 15 min on ice. Cells were then washed and incubated with allogeneic IgG (2 μg per 1×10^6 cells) for 30 min on ice. Cells were centrifuged at 5,000 r.p.m. for 10 min, and the supernatants were concentrated by 50 kDa centrifugal filters (Amicon) before being incubated with 1×10^5 tumour cells.

Membrane protein extraction. For native membrane protein extraction, B16F10 cells were scraped in cold PBS and pelleted at 400*g* for 5 min at 4 °C. The cell pellet was washed twice in cold PBS, resuspended in 10 mM HEPES pH 7.4 and incubated on ice for 10 min. Cells were pelleted and the buffer was removed. The cell pellet was resuspended in 10 ml of SEAT buffer (10 mM triethanolamine/acetic acid, 1 mM EDTA pH 8.0, 250 mM sucrose, protease inhibitor cocktail) and homogenized with 20 strokes of a dounce homogenizer. The sample was spun at 900*g* for 6 min to collect the post-nuclear supernatant (PNS). The PNS was spun at 100,000*g* for 60 min at 4 °C to harvest a membrane pellet, which was then resuspended in 4 ml membrane extraction buffer (MEB) containing 50 mM Tris-HCl pH 8.0, 150 mM NaCl, 1% NP-40, 1 mM DTT, 10% glycerol, 1 mM NaF, and protease inhibitor cocktail. After incubation for 2 h at 4 °C, the membrane extract was clarified by centrifugation at 100,000*g* for 30 min at 4 °C. For denatured membrane protein extraction, the membrane pellet was resuspended in 500 μl Radio-Immuno-Precipitation Assay buffer (RIPA, Sigma) and lysed with a 25G needle syringe. Lysates were incubated at 4 °C for 1 h and spun at 100,000*g*, 30 min, 4 °C. Supernatant containing detergent solubilized membrane proteins was collected and boiled for 5 min at 95 °C. Deglycosylation of membrane proteins was performed using a commercial kit (New England Biolabs, Ipswich, Massachusetts) according to the manufacturer's instructions. Isolation of cell-membrane proteins was repeated three independent times and the running pattern of precipitated proteins was compared on SDS–PAGE.

Immunoprecipitation and mass spectrometry. Immunoprecipitation was set up with 20 mg membrane extract and 50 μg of syngeneic or allogeneic IgG coupled to protein G magnetic beads and incubated for 16 h at 4 °C. Beads were washed thrice with MEB and bound protein complexes were eluted with 2× Laemmli buffer. The eluted sample was subjected to SDS–PAGE on a 4–12% Bis-Tris gel followed by GelCode blue staining (Thermo Scientific) to visualize protein bands. Protein bands were excised, digested with trypsin and analysed (MS Bioworks) using a nano LC/MS/MS with a NanoAcquity HPLC system (Waters) interfaced to a Q Exactive (Thermo Fisher). The mass spectrometer was operated in data-dependent mode, with MS and MS/MS performed in the Orbitrap at 70,000 FWHM and 17,500 FWHM resolution, respectively. The 15 most abundant ions were selected for MS/MS. The data were processed with the Mascot Server (Matrix Science). Mascot DAT files were parsed into the Scaffold software for validation, filtering and to create a non-redundant list per sample. Data were filtered at 1% protein and peptide FDR, requiring at least two unique peptides per protein. Mass spectrometry analysis of precipitated proteins was performed once.

Native gel and tumour cell GPNMB staining. Recombinant mouse GPNMB (R&D) was mixed with native loading buffer (16% glycerol, 1% Trypan blue and 50 mM pH 7.0 Tris-HCl) and 62.5 and 125 ng per well was run for 2 h in Novex NativePAGE Bis-Tris gel system (Life Technologies) on ice. Bands were transferred to a nitrocellulose membrane and incubated overnight with 10 μg ml^{-1} mouse IgG, or with 1 μg ml^{-1} rabbit polyclonal IgG anti-mouse GPNMB (cat. no. S-24 sc-133634, Santa Cruz). The membranes were washed, incubated for 45 min with goat anti-mouse IgG light-chain-specific antibodies conjugated to HRP (Pierce), developed with SuperSignal West Femto Substrate (Pierce), and exposed together for imaging.

For FACS staining of GPNMB on tumour cells, 1×10^5 B16 or LMP cells were incubated with 2 μg rabbit polyclonal anti-mouse GPNMB (Santa Cruz) for 30 min, washed twice and incubated for 20 min with PE-conjugated donkey anti-rabbit or goat anti-mouse antibodies, respectively (both from eBioscience). FACS measurements were repeated three independent times in biological duplicates.

***In vivo* tumour models.** For tumour challenge studies, 2×10^5 and 5×10^4 LMP or B16 tumour cells, respectively, were injected subcutaneously (s.c.) above the right flank, and tumour development was measured twice a week with calipers. In some experiments, 1–2 $\times 10^6$ tumour cells were labelled with 25 μM CFSE according to the manufacturer's instructions (Invitrogen). Tumour challenge experiments were repeated independently at least 8 times with 4 mice per group. For prophylactic immunization, mice were injected twice s.c., 7 days apart, with 2×10^6 DCs or monocytes that were loaded with tumour lysates or immune complexes. This was independently repeated 3 times with 4 mice per group. For tumour recurrence studies, 2×10^5 tumour cells were injected s.c. above the right flank, and the size of growing tumours was measured using calipers. When tumours reached 45–55 mm^2 for LMP and 12–16 mm^2 for B16, mice were anaesthetized and visible macroscopic tumour was surgically removed. Resected tumours were enzymatically digested with 0.1 mg ml^{-1} of DNase I (Sigma) and 5 mg ml^{-1} collagenase IV (Sigma) in HBSS. Cells were then fixed in 2% paraformaldehyde for 20 min, washed extensively in PBS and coated for 30 min with syngeneic or allogeneic antibodies. In some experiments, tumour cells were coated with mouse anti-mouse anti-H2-K^b (2μg/1x10^5 cells) or its isotype control (C1.18.4, both from BioXcell). Antibody-coated tumour cells were then washed and added to DC cultures. After overnight incubation, DCs were washed and 2.5×10^6 were injected s.c. to tumour-resected mice one day after the tumours were removed, adjacent to the site of tumour resection. This experiment was repeated independently at least 3 times with 4 mice per group. For *in vivo* tumour treatments, a combination of 2 μg TNFα (Peprotech) and 100 μg agonistic anti-CD40 (FGK4.5, BioXcell), 5 μg recombinant CD40L (PeproTech), 5 μg CD28 (R&D Systems, Minneapolis, Minnesota), 5 μg LPS or 200 μg poly(I:C) (Invivogen), and 400 μg mouse allogeneic or syngeneic IgG or anti-GP-NMB (Santa Cruz), was injected twice (2 days apart) directly into tumours. Experiments were repeated independently at least 5 times with 4–5 mice per group. For treatment of the $Braf^{V600E}$ melanoma model, mice were injected twice (2 days apart) in 2 cycles, one week apart, with 1 mg IgG derived from CD-1 mice along with TNFα and anti-CD40 once the largest tumour nodule reached 16 mm^2. For metastasis experiments, 1×10^5 4T1 cells were injected into the mammary fat pad of syngeneic Balb/c mice. After 14–16 days, once tumours metastasized into the draining lymph node, the primary tumour nodules were injected twice (2 days apart) in 2 cycles, one week apart, with 1 mg IgG derived from CD-1 mice along with TNFα and anti-CD40. Experiments were repeated independently at least 3 times with 3–5 mice per group.

***In vivo* binding of PE-labelled allogeneic IgG.** Allogeneic antibodies were fluorescently labelled with PE using Lightning-Link kits according to the manufacturer's instructions (Innova Biosciences Ltd, Cambridge, UK). Subsequently, 5 μg of labelled allogeneic IgG was injected intratumorally alone or with TNFα and anti-CD40. After 2 h, tumours were enzymatically digested to obtain a single cell suspension and the PE levels were analysed by flow cytometry along with lineage markers.

Covalent binding of syngeneic antibodies to tumour cells. Syngeneic IgG was cross-linked to primary amines of B16 cell surface proteins using sulfo-LC-SPDP (sulfosuccinimidyl 6-(3′-[2-pyridyldithio]-propionamido) hexanoate, Pierce) according to the manufacturer's instructions. Briefly, both the antibodies and cells were initially treated with sulfo-LC-SPDP to label primary amines. Next, disulfide bonds in syngeneic IgG were reduced by treatment with DTT. Finally, the reduced syngeneic IgG was incubated with SPDP-labelled B16 cells and the level of binding was later assessed by flow cytometry. Experiments were repeated independently 3 times with 4 mice per group.

***In vivo* cell depletion.** Depletion of $CD4^+$ and $CD8^+$ T cells was achieved by intraperitoneal (i.p.) injection of 500 μg per mouse GK1.5 (anti-CD4) and YST-169.4 (anti-CD8) monoclonal antibodies (both from BioXcell, West Lebanon), respectively, 3 days before tumour inoculation and every 3 days thereafter. T-cell depletion experiments were repeated independently 3 times for each depletion antibody with 3–4 mice per group. In some experiments, B16-bearing mice were injected with 500 μg per mouse anti-CD8 or anti-CD4 2 days before their treatment with antibodies+TNFα+anti-CD40 and once a week thereafter. These T-cell depletion experiments were repeated independently 2 times for each depletion antibody with 5 mice per group. For B cell depletion, 300 μg per mouse anti-CD19 (1D3) and 300 μg per mouse anti-B220 (RA3.3A1/6.1) (both from BioXcell) were injected i.p. three weeks before tumour inoculation and every 5 days thereafter. B-cell depletion experiments were repeated independently 3 times with 3–5 mice per group. For NK cell depletion, mice were injected i.p. with 50 μl anti-asialo (GM1) polyclonal antibody (Wako Chemicals, Richmond, Virginia), or with 200 μg anti-NK1.1 (PK136) (BioXCell) on days −2, 0, 4 and 8 relative to tumour challenge. Individual mice were bled on days 0, 7, 14 and 21 and the levels of $NK1.1^+/CD3\varepsilon^-$ cells were determined by flow cytometry to confirm depletion. NK cell depletion experiments were repeated independently 3 times with anti-asialo depletion antibody with 3–5 mice per group.

Adoptive transfer. Mice were injected i.v. with 1 mg per mouse of syngeneic or allogeneic IgG or IgM one day before tumour challenge and once again with tumour injection. For T-cell transfer, splenic $CD4^+$ and $CD8^+$ T cells were negatively selected using a murine enrichment kit (Stem Cell Technologies) and at least 5×10^6 cells were injected i.v. to recipient mice one day before tumour challenge. T-cell adoptive transfer experiments were repeated independently 3 times for each T cell subset with 3–5 mice per group. Prior to their transfer, tumour-associated cell subsets were enriched as follows: TADCs were isolated by enrichment of $MHCII^+$ cells on magnetic beads (Miltenyi) and subsequent sorting of $Ly6C^-CD11c^+CD64^{dim}$ by FACS. Tumour macrophages were enriched with $CD11b^+$ magnetic beads (Miltenyi) followed by sorting of $Ly6C^-CD64^{hi}$ cells. B cells were enriched with $CD19^+$ magnetic beads (Miltenyi). NK cells were enriched with $NK1.1^+$ magnetic beads (Miltenyi), and mast cells were enriched with c-kit^+ magnetic beads (Miltenyi). For each cell subset, 2×10^6 cells were

injected s.c. into naive mice 3 days before being challenged with 5×10^4 B16 tumour cells. Transfer experiments for each cell type were repeated 3 times independently with 3–5 mice per group.

T-cell proliferation. 3×10^4 DCs were co-cultured with 3×10^5 MACS-enriched $CD4^+$ T cells (Miltenyi, Germany) from spleens of LMP- or B16-immunized mice. After 6 days, cells were pulsed with [^{3}H]thymidine (1 μCi per well) and cultured for an additional 18 h before being harvested in a Harvester 400 (Tomtec). Radioactivity was measured by a 1450 MicroBeta counter (LKB Wallac). T-cell proliferation was repeated 5 times with 3 biological replicates and 6 technical replicates for each.

***In vivo* BrdU incorporation.** Tumour-challenged mice were injected i.p. every day with 1 mg of 5-bromo-2-deoxyuridine (BrdU) in 200 μl PBS. At several time points, mice were killed and single cell suspensions were prepared from BM, lymph nodes and tumour tissues. Cells were then stained for lineage markers followed by intracellular staining with FITC-conjugated anti-BrdU antibody according to manufacturer's instructions (BD Pharmingen) and analysed by flow cytometry. Experiments were repeated independently 3 times with 3–5 mice per group.

Immunofluorescence. DCs or monocytes were incubated on glass-bottom culture plates (In vitro Scientific) with CFSE-labelled tumour cells with or without antibodies overnight. Cells were gently washed with PBS (Gibco), fixed for 20 min with 2% paraformaldehyde and permeabilized with 0.5% saponin (Sigma). Samples were blocked with 10% non-immune goat serum and stained with Alexa-conjugated anti-mouse IgG and IgM (Invitrogen 1:100) and anti-mouse I-Ab (BD Biosciences, 1:100). DC immunostainings were independently repeated at least 3 times in biological duplicates and 3 fields were documented in each slide.

Immunohistochemistry. Specimens were fixed in 4% paraformaldehyde, equilibrated in a 20% sucrose solution and embedded in frozen tissue matrix (Tissue-Tek OCT, Torrance, California). Slides were cut to 5 μm, blocked with 10% non-immune goat serum and stained with goat anti-mouse IgG (Invitrogen 1:100) and anti-mouse IgM (II/41 eBioscience, 1:100). Sections were examined under a Zeiss Laser Scanning Confocal Microscope. Images were collected using a Zeiss 700 confocal laser scanning microscope, and analysed using ZEN software (Carl Zeiss Microscopy). Tumour immunostainings were repeated independently at least 3 times in biological duplicates and 3 fields were captured for each slide.

Statistics. No statistical methods were used to predetermine sample size, but sample size was chosen such that statistical significance could be achieved using appropriate statistical tests (for example, ANOVA) with errors approximated from previously reported studies. A non-parametric Mann–Whitney *U* test was performed in Prism (GraphPad Software, Inc.) to analyse experimental data, unless otherwise stated. Phospho-specific flow cytometry data were transformed by taking the inverse hyperbolic sine (arcsinh), and ratios were taken over the corresponding baseline (unstimulated) value[31]. No blinded experiments were performed. No samples were excluded from analyses. *P* values indicate significance of the difference between experimental and control (CT) values. $*P < 0.05$; $**P < 0.01$. Error bars represent ± s.e.m.

31. Irish, J. *et al.* B-cell signaling networks reveal a negative prognostic human lymphoma cell subset that emerges during tumor progression. *Proc. Natl. Acad. Sci. USA* **29,** 12747–12754 (2010).

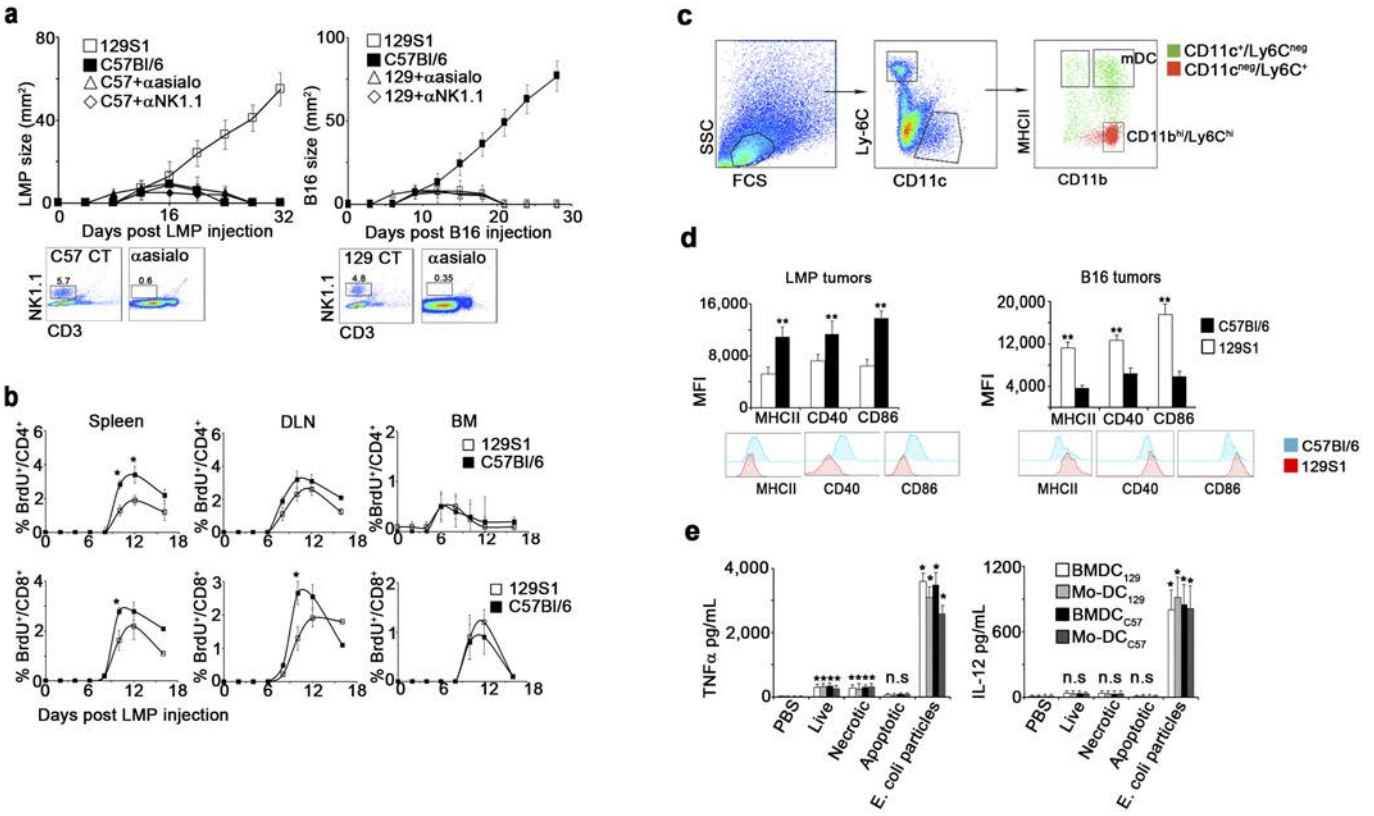

Extended Data Figure 1 | DCs acquire an activated phenotype in response to allogeneic tumours injected *in vivo*, but not when co-cultured *in vitro*. **a**, LMP (left) and B16 (right) growth in 129S1, C57BL/6, or allogeneic hosts pre-treated with anti-asialo-GM1 or anti-NK1.1 antibodies ($n = 6$, 3 independent experiments). Shown are representative plots of NK cells in the blood before tumour challenge. **b**, BrdU incorporation by $CD4^+$ T cells (top) and $CD8^+$ T cells (bottom) in lymphoid organs of 129S1 and C57BL/6 LMP-bearing mice ($n = 8$, 3 independent experiments). **c**, Representative flow cytometric analysis of $CD11b^{hi}Ly6C^{hi}$ myeloid cells and mature DCs (mDCs) on day 10 after C57BL/6 mice were inoculated with B16 tumour cells. **d**, Flow cytometric analysis of $Ly6C^-CD11c^+MHCII^+$ cells from LMP-bearing mice (left) and B16-bearing mice (right). Histograms show representative expression levels of co-stimulatory molecules on DCs from C57BL/6 and 129S1 mice ($n = 8$, 3 independent experiments). **e**, IL-12 (right) and TNFα (left) in the supernatants of syngeneic BMDCs, syngeneic blood monocyte-derived (Mo) DCs, allogeneic BMDCs or Mo-DCs incubated with live, frozen-thawed (necrotic), or mitomycin-C-treated (apoptotic) LMP cells or *E. coli* BioParticles overnight ($n = 8$, 4 independent experiments). Shown are the mean values ± s.e.m. $^*P < 0.05$; $^{**}P < 0.01$.

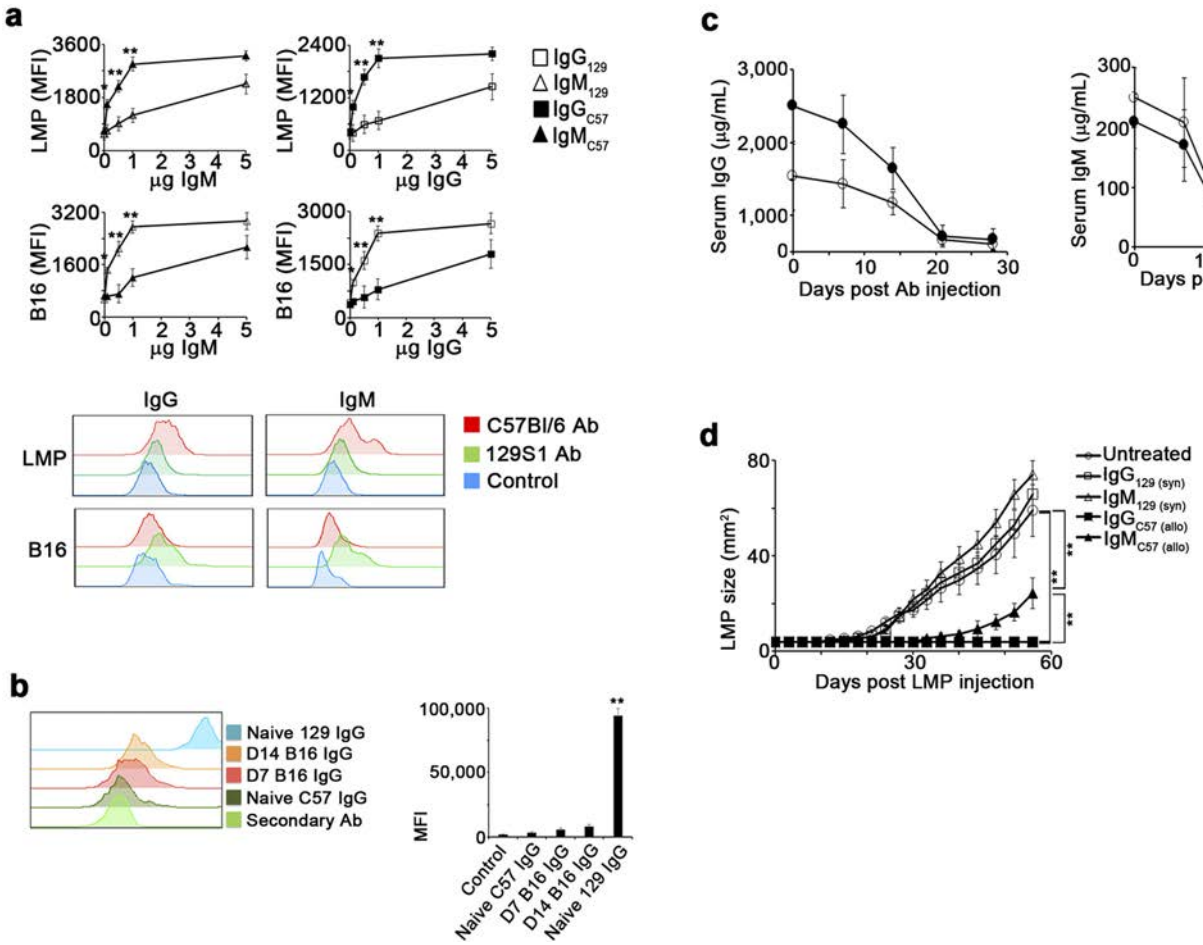

Extended Data Figure 2 | Allogeneic hosts have a much higher titre of tumour-binding antibodies compared to syngeneic hosts a, Flow cytometric analysis of the binding of various concentrations of IgG from 129S1, IgM from 129S1, IgG from C57BL/6 and IgM from C57BL/6 mice to LMP and B16 cells. The lower panel shows a representative histogram of IgG (left) or IgM (right) binding after incubation of 1 μg of C57BL/6 or 129S1 antibodies with 1×10^5 LMP (upper) or B16 (lower) cells ($n = 8$, 4 independent experiments). **b**, The left panel shows a representative histogram of the MFI of IgG after incubation of 2 μg of either control antibody (secondary Ab) or IgG from the serum of naive C57Bl/6 mice, B16-bearing C57BL/6 mice on day 7, B16-bearing C57BL/6 mice on day 14 or naive 129S1 mice with 1×10^5 B16 cells ($n = 6$, 4 independent experiments). Right graph shows MFI of the binding of 2 μg of each IgG to 1×10^5 B16 cells. **c**, Serum levels of IgG (left) and IgM (right) in C57BL/6 and 129S1 mice following i.p injection with anti-B220 and anti-CD19 antibodies ($n = 8$, 3 independent experiments). **d**, LMP tumour size in naive 129S1 mice injected with allogeneic IgG, allogeneic IgM, syngeneic IgG or syngeneic IgM on days −1 and 0 relative to tumour injection ($n = 6$, 3 independent experiments). Shown are the mean values ± s.e.m. $*P < 0.05$; $**P < 0.01$.

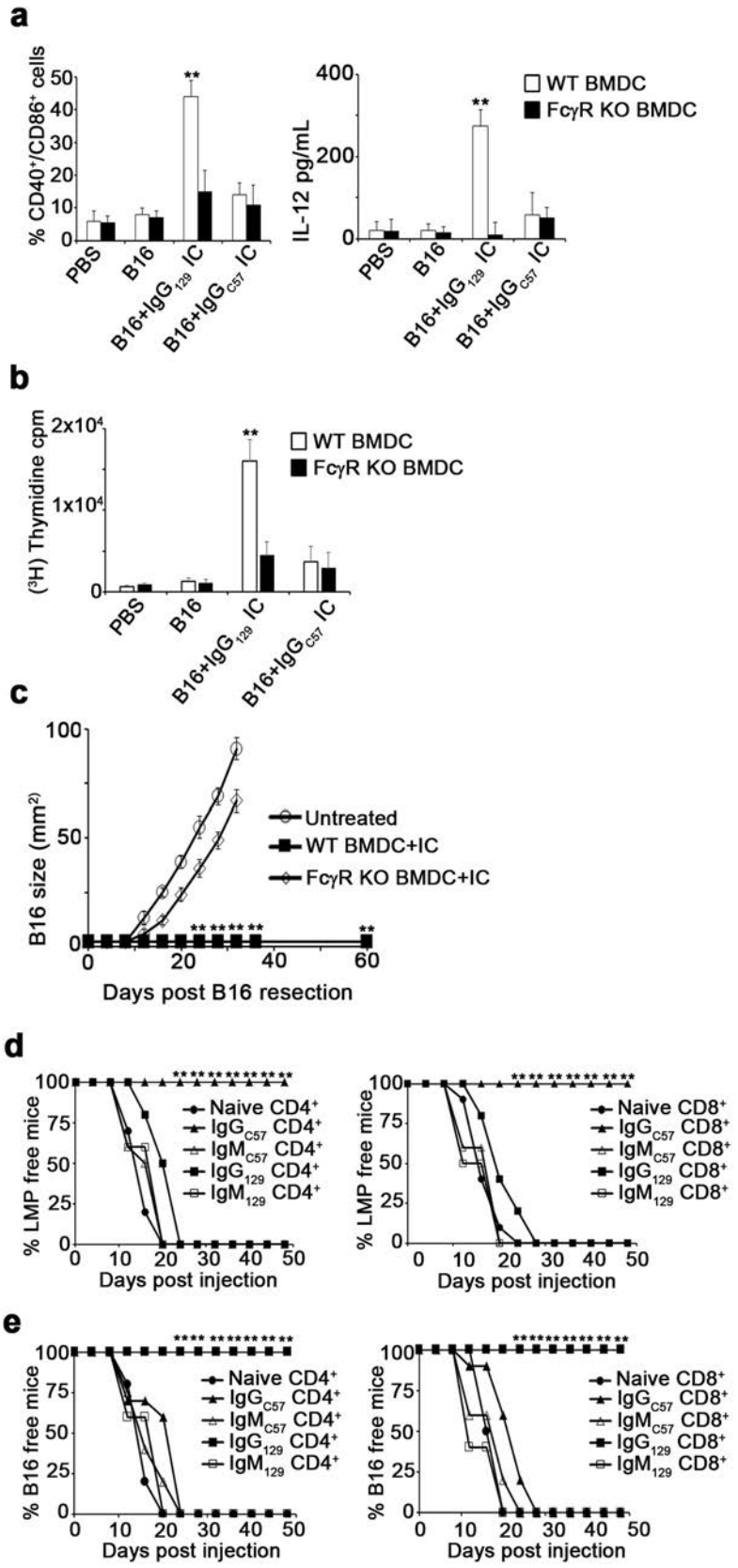

Extended Data Figure 3 | Activation of BMDCs with immune complexes induces transferable T-cell immunity. **a**, Mean levels of CD40 and CD86 expression (left) and IL-12 secretion (right) in BMDCs from C57BL/6 (WT) and FcγR KO mice activated with IgG-IC overnight ($n = 6$, 10 independent experiments). **b**, Proliferation of $CD4^+$ T cells cultured with BMDCs from C57BL/6 and FcγR KO mice loaded with IgG-IC ($n = 4$, 5 independent experiments). **c**, Tumour recurrence in untreated mice, mice treated with WT BMDCs loaded with IgG-IC, or mice treated with FcγR KO BMDCs loaded with IgG-IC ($n = 8$, 3 independent experiments). **d**, **e**, Percentages of tumour-free mice after adoptive transfer of 5×10^6 splenic $CD4^+$ T cells (left graph) or $CD8^+$ T cells (right graph) from naive mice, or from LMP (**d**)- or B16 (**e**)-resected mice treated with DCs + IgG_{C57} IC, DCs + IgM_{C57} IC, DCs + IgG_{129} IC, or DCs + IgM_{129} IC, and subsequently challenged with LMP (**d**) or B16 (**e**) ($n = 6$, 3 independent experiments). Shown are the mean values ± s.e.m. $^{**}P < 0.01$.

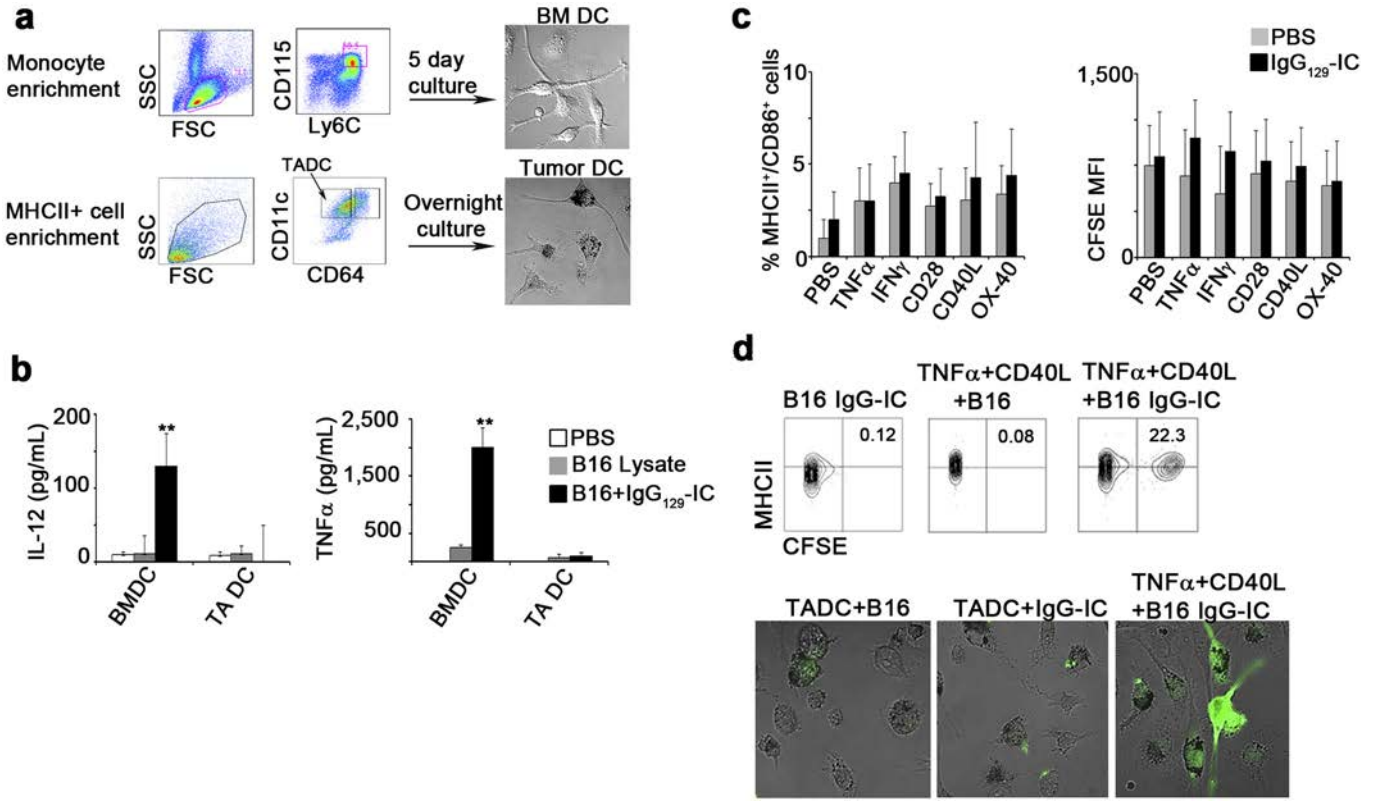

Extended Data Figure 4 | Tumour-associated DCs do not respond to immune complexes. **a**, Sorting and culture schema of DCs from BM and tumour. **b**, Mean levels of IL-12 (left) and TNFα (right) in the supernatants of DCs cultured overnight in medium alone, with B16 lysates, or with alloIgG-IC ($n = 6$, 4 independent experiments). **c**, Percentage of $MHCII^+CD86^+$ cells (left) or CFSE levels (right) in tumour-associated DCs after overnight activation with PBS or CFSE-labelled alloIgG-IC with or without stimulatory molecules ($n = 12$, 10 independent experiments). **d**, Representative flow cytometric analysis and confocal images from one out of three independent experiments of B16-derived DCs cultured overnight with CFSE-labelled fixed B16 cells ($n = 8$, 10 independent experiments). Shown are the mean values ± s.e.m. $^*P < 0.05$; $^{**}P < 0.01$.

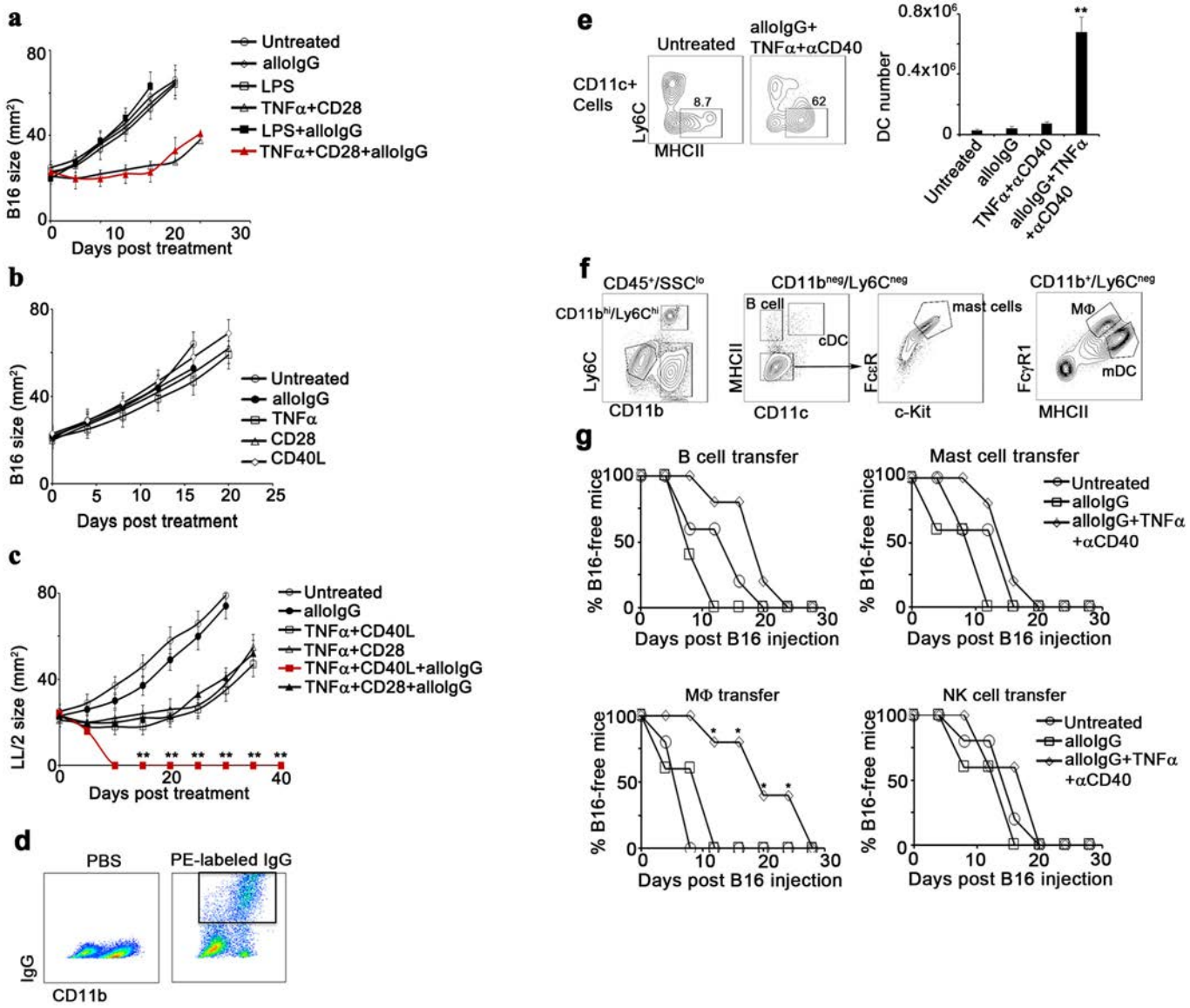

Extended Data Figure 5 | Tumour DCs from mice treated with alloIgG + adjuvant can internalize immune complexes and transfer immunity. **a**, B16 tumour size in C57BL/6 mice left untreated or injected intratumorally with 129S1 allogeneic IgG, LPS, TNFα + CD28, LPS + allogeneic IgG or TNFα + CD28 + allogeneic IgG ($n = 15$, 3 independent experiments). **b**, B16 tumour size in C57BL/6 mice left untreated or injected intratumorally with 129S1 allogeneic IgG, TNFα, CD28, or CD40L ($n = 12$, 3 independent experiments). **c**, Lewis lung carcinoma (LL/2) tumour size in C57BL/6 mice left untreated, or injected intratumorally with 129S1 allogeneic IgG, TNFα + CD40L, TNFα + CD28, TNFα + CD40L + 129S1 allogeneic IgG or TNFα + CD28 + 129S1 IgG ($n = 8$, 2 independent experiments). **d**, Representative flow cytometric analysis from one out of three independent experiments of IgG binding total myeloid cells in B16 tumour-bearing mice 3 h after intratumoral injection of PBS or 5 μg PE-labelled allogeneic IgG. **e**, Total numbers of $CD11c^+$ cells in the draining lymph nodes of B16 tumour-bearing mice 4 days after treatment ($n = 6$, 3 independent experiments). **f**, Gating and sorting strategy of immune cell populations infiltrating B16 tumours. **g**, B16 growth in mice vaccinated with 2×10^6 B cells, mast cells, macrophages or NK cells from B16 tumours untreated, or injected with allogeneic IgG or allogeneic IgG + TNFα + anti-CD40 ($n = 6$, 3 independent experiments). Shown are the mean values ± s.e.m. $^*P < 0.05$; $^{**}P < 0.01$.

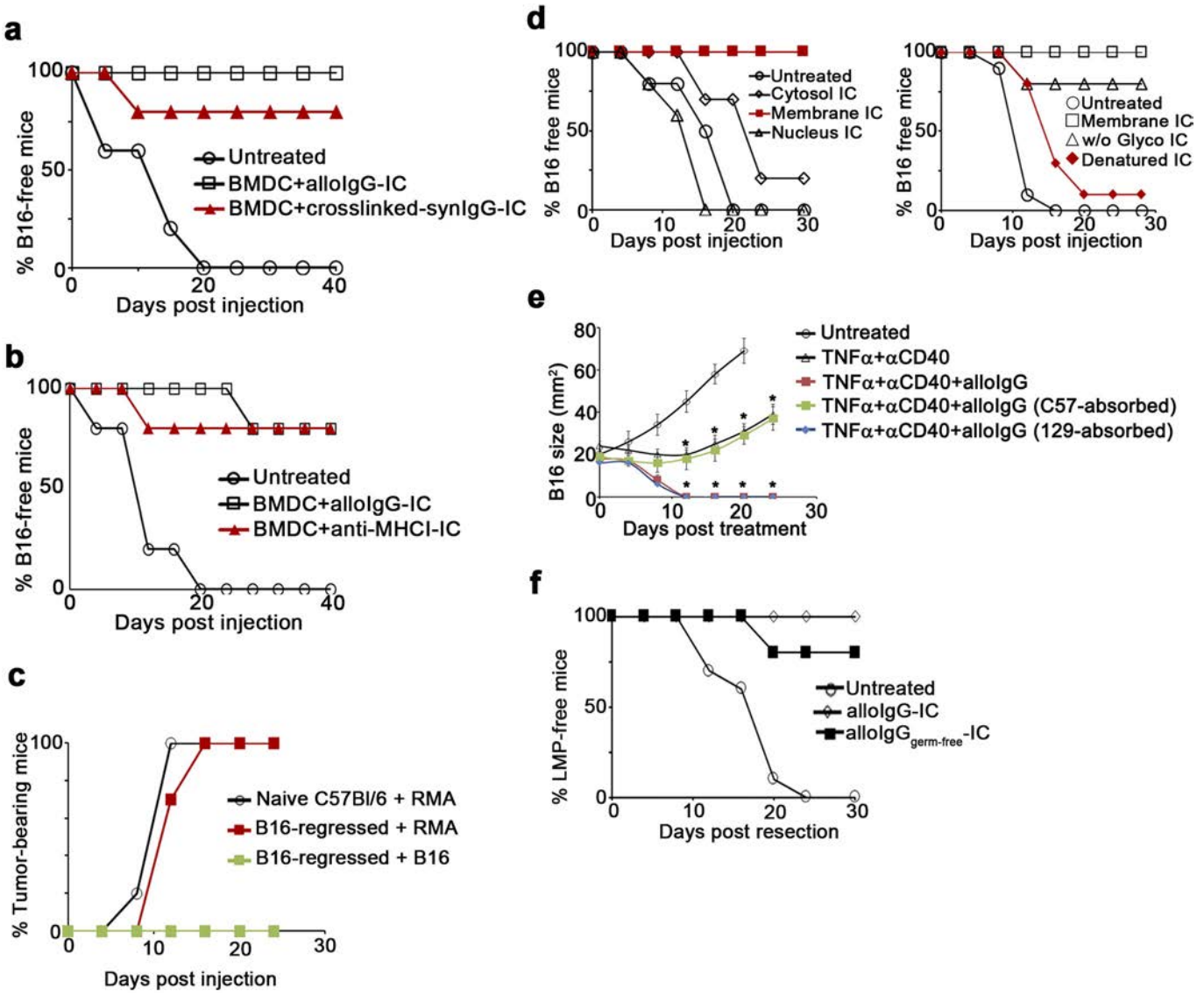

Extended Data Figure 6 | Allogeneic IgG recognises non-mutated cell membrane proteins on tumour cells. **a**, B16 frequency in mice untreated, or treated with BMDCs loaded with intact B16 cells coated with allogeneic IgG, or with intact B16 cells cross-linked to syngeneic IgG ($n = 8$, 3 independent experiments). **b**, B16 tumour frequency in mice untreated or treated with BMDCs loaded with intact B16 cells coated with allogeneic IgG or with intact B16 coated with monoclonal IgG against MHC-I ($n = 8$, 3 independent experiments). **c**, RMA tumour growth following inoculation with 2.5×10^5 tumour cells in naive C57BL/6 mice, or in C57BL/6 mice in which B16 tumours had completely regressed after treatment with allogeneic IgG + TNFα + anti-CD40. Also shown is the lack of B16 tumour growth in C57BL/6 mice that were re-challenged with 2×10^5 B16 tumour cells following the regression of this tumour after treatment with allogeneic IgG + TNFα + anti-CD40 ($n = 8$, 2 independent experiments). **d**, Left: tumour frequency in mice untreated or treated with DCs loaded with immune complexes formed with allogeneic IgG and cytosolic tumour proteins, nuclear tumour proteins or membrane tumour proteins. Right: tumour frequency in mice untreated, treated with DCs loaded with immune complexes formed from allogeneic IgG and membrane proteins, membrane proteins without O- and N-glycans, or heat-denatured membrane proteins ($n = 5$, 3 independent experiments). **e**, B16 tumour growth in C57BL/6 mice untreated, or injected with TNFα + anti-CD40, TNFα + anti-CD40 + allogeneic IgG, or TNFα + anti-CD40 and allogeneic IgG absorbed on normal cells of the IgG-donor background (blue diamonds) or on normal cells of the tumour background (green squares) ($n = 6$, 3 independent experiments). **f**, Tumour recurrence rates after resection in mice left untreated, treated with 2×10^6 DCs loaded with IgG-IC from conventionally raised C57BL/6, or with 2×10^6 DCs loaded with IgG-IC from gnotobiotic C57BL/6 mice ($n = 6$, 2 independent experiments). Shown are the mean values ± s.e.m. $^*P < 0.05$; $^{**}P < 0.01$.

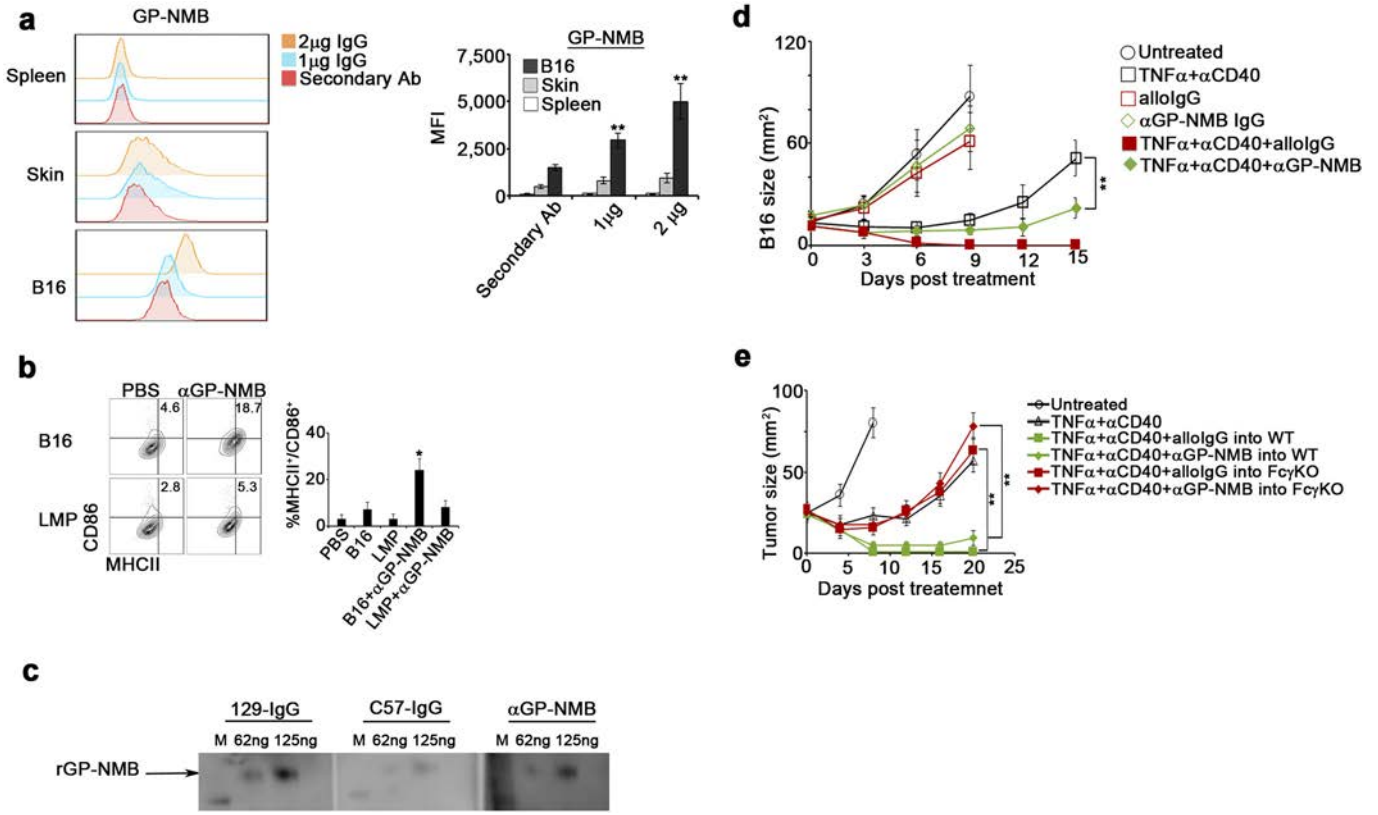

Extended Data Figure 7 | Allogeneic hosts have a higher titre of anti-GP-NMB IgG, which can be used to induce tumour immunity. **a**, Representative flow cytometric analysis and quantification of binding of anti-IgG secondary antibody alone, 1 μg anti-GPNMB or 2 μg GPNMB per 1×10^5 B16 cells, normal skin cells, or normal spleen cells ($n = 6$, 3 independent experiments). **b**, Percentage of $MHCII^+CD86^+$ BMDCs following overnight activation with untreated LMP or B16 tumour cells, or with tumour cells coated with anti-GPNMB (2 μg per 1×10^5 tumour cells) ($n = 8$, 3 independent experiments). **c**, Western blot of recombinant GPNMB (62.5 ng and 125 ng) performed with 10 μg ml^{-1} of IgG from naive 129S1 mice, naive C57BL/6 mice, or 1 μg ml^{-1} anti-GPNMB (2 independent experiments). **d**, B16 tumour size in mice untreated or treated with TNFα + anti-CD40, allogeneic IgG, anti-GPNMB IgG, TNFα + anti-CD40 + allogeneic IgG, or with TNFα + anti-CD40 + anti-GPNMB ($n = 8$, 3 independent experiments). **e**, B16 tumour size in C57Bl/6 WT mice untreated or treated with TNFα + anti-CD40, TNFα + anti-CD40 + allogeneic IgG, or with TNFα + anti-CD40 + anti-GPNMB, or in FcγR KO mice treated with TNFα + anti-CD40 + allogeneic IgG, or with TNFα + anti-CD40 + anti-GPNMB ($n = 8$, 3 independent experiments). Shown are the mean values ± s.e.m. $*P < 0.05$; $**P < 0.01$.

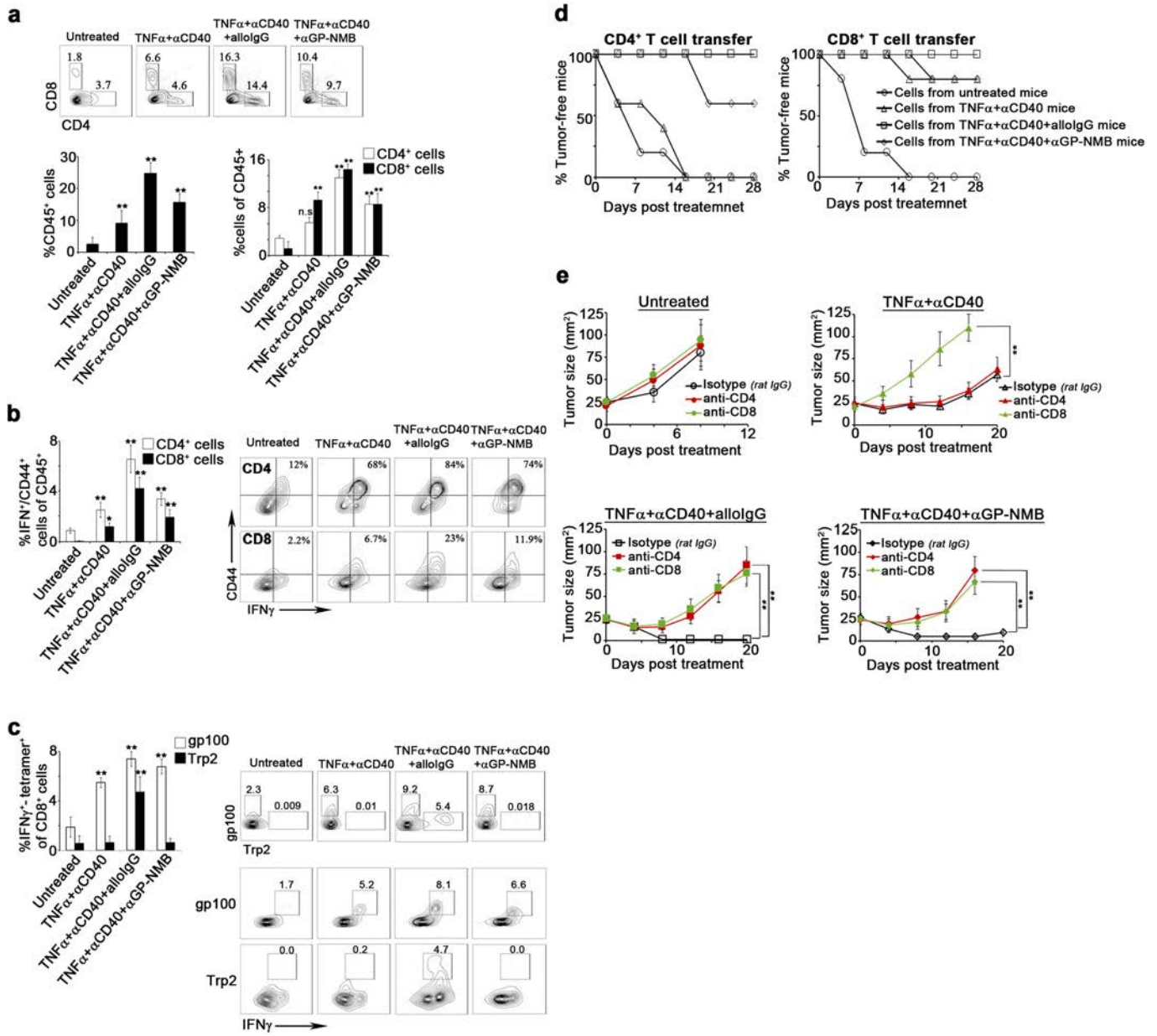

Extended Data Figure 8 | AlloIgG and anti-GPNMB IgG induce tumour-reactive T-cell infiltration and activation. **a**, Representative flow cytometry plots of $CD4^+$ and $CD8^+$ cells in B16 tumours 6 days after treatment. Left: percentage of $CD45^+$ cells infiltrating B16 tumours 15–17 days after s.c. inoculation or 6 days after treatment. Right: percentage of $CD4^+$ and $CD8^+$ cells among tumour-infiltrating $CD45^+$ cells ($n = 10$, 3 independent experiments). **b**, Percentages of CD44 and IFNγ co-expressing $CD4^+$ and $CD8^+$ cells among tumour-infiltrating $CD45^+$ cells 6 days after treatment or 15 days following s.c. inoculation ($n = 10$, 3 independent experiments) **c**, Frequency of IFNγ-expressing T cells that recognize gp100 and Trp2 among day 6 post-treatment tumour-infiltrating $CD8^+$ cells. Gate shown: $CD8^+$ T cells ($n = 10$, 3 independent experiments). **d**, Percentage of tumour-free mice following adoptive transfer of T cells from day 6 post-treatment B16 tumour-bearing mice untreated, treated with TNFα + anti-CD40, with TNFα + anti-CD40 + allogeneic IgG, or with TNFα + anti-CD40 + anti-GPNMB ($n = 9$, 3 independent experiments). **e**, Upper left: B16 tumour growth in untreated C57BL/6 mice injected with rat IgG, with rat anti-CD4, or with rat-CD8. Upper right: B16 tumour growth in C57BL/6 mice treated with TNFα + anti-CD40 and injected with rat IgG, with rat anti-CD4, or with rat-CD8. Lower left: B16 growth in C57BL/6 mice treated with TNFα + anti-CD40 + allogeneic IgG and injected with rat IgG, with rat anti-CD4, or with rat-CD8. Lower right: B16 growth in C57BL/6 mice treated with TNFα + anti-CD40 + anti-GPNMB and injected with rat IgG, with rat anti-CD4, or with rat-CD8 ($n = 9$, 3 independent experiments). Shown are the mean values ± s.e.m. from three independent experiments. $^*P < 0.05$; $^{**}P < 0.01$.

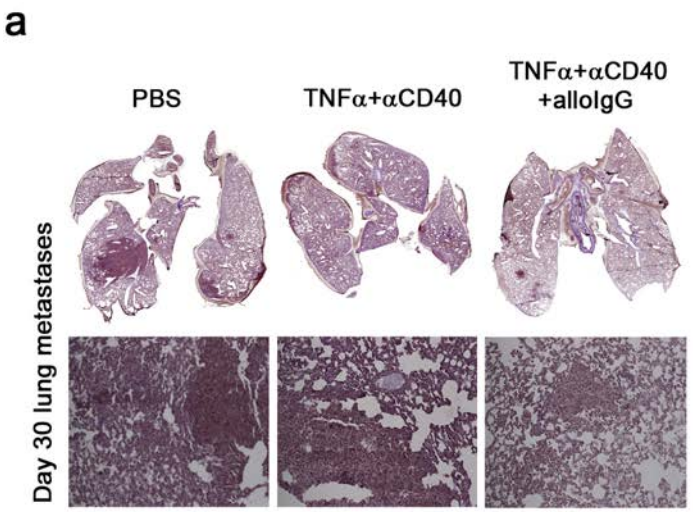

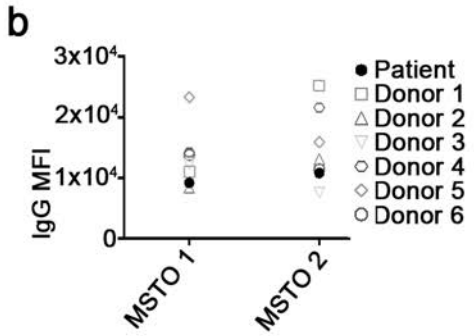

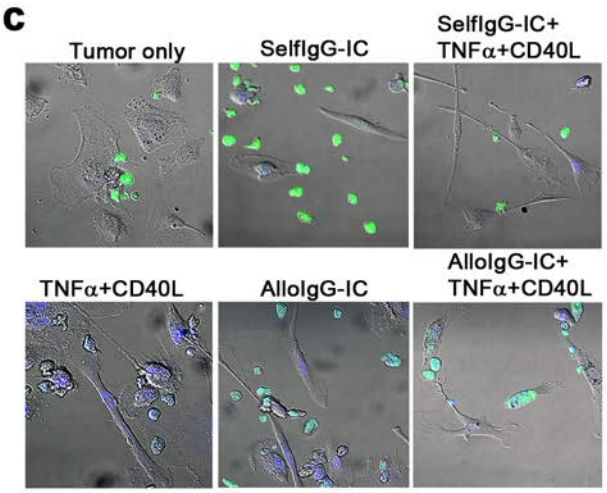

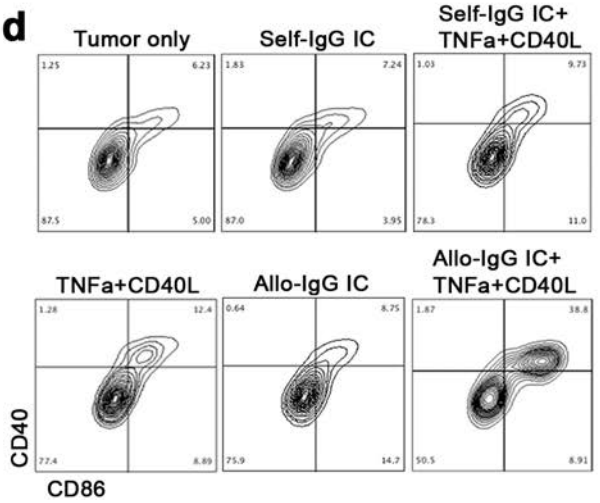

Extended Data Figure 9 | AlloIgG can activate human tumour DCs to process autologous tumour cells. **a**, Representative haematoxylin and eosin sections of lung metastases on day 30 from one out of three independent experiments performed (original magnification, 10×). **b**, MFI of tumour cells from MSTO-resected patients coated with autologous IgG or IgG from healthy donors ($n = 2$ in technical triplicates). **c**, **d**, Wide-field microscopy (**c**) and flow cytometry plots (**d**) of TADCs from a lung carcinoma patient incubated overnight with autologous CFSE-labelled tumour cells (green) coated with self IgG or allogeneic IgG derived from a pool of 10 donors (1 μg per 2×10^5 cells) and in the presence of 50 ng ml^{-1} TNFα and 1 μg ml^{-1} CD40L ($n = 2$ in technical triplicates). Shown are the mean values ± s.e.m. from two independent experiments. $^*P < 0.05$; $^{**}P < 0.01$.

Extended Data Table 1 | Allogeneic IgG binds numerous membrane tumour proteins

a. Proteins enriched by alloIgG

	Identified Proteins	Accession Number	C57 SpC	129 SpC	C57 SAF	129 SAF	C57 NSAF	129 NSAF	C57/129 ratio
Endoplasmic reticulum membrane									
1	Transmembrane protein 93	sp|Q9CQW0|TMM93_MOUSE	0	2	0	0.166667	0	0.0007367	2
2	Endoplasmic reticulum-Golgi intermediate compartment protein 3	sp|Q9CQE7|ERGI3_MOUSE	0	2	0	0.046512	0	0.00020559	2
3	Reticulon-4	sp|Q99P72|RTN4_MOUSE	0	2	0	0.015748	0	6.9609E-05	2
4	Uncharacterized protein C12orf41 homolog	sp|Q8BQR4|CL041_MOUSE	0	2	0	0.037037	0	0.00016371	2
5	Erlin-2	sp|Q8BFZ9|ERLN2_MOUSE	0	2	0	0.052632	0	0.00023264	2
6	Transitional endoplasmic reticulum ATPase	sp|Q01853|TERA_MOUSE	0	2	0	0.022472	0	9.933E-05	2
7	Dolichyl-diphosphooligosaccharide--protein glycosyltransferase subunit DAD1	sp|P61804|DAD1_MOUSE	0	2	0	0.166667	0	0.0007367	2
8	Calnexin	sp|P35564|CALX_MOUSE	0	2	0	0.029851	0	0.00013195	2
9	Calumenin	sp|O35887|CALU_MOUSE	0	2	0	0.054054	0	0.00023893	2
10	Vesicle-associated membrane protein-associated protein A	sp|Q9WV55|VAPA_MOUSE	0	3	0	0.107143	0	0.00047359	3
11	Mannosyl-oligosaccharide glucosidase	sp|Q80UM7|MOGS_MOUSE	0	3	0	0.032609	0	0.00014414	3
12	Neutral alpha-glucosidase	sp|Q8BHN3|GANAB_MOUSE	0	3	0	0.028037	0	0.00012393	3
13	ERO1-like protein alpha	sp|Q8R180|ERO1A_MOUSE	0	5	0	0.092593	0	0.00040928	5
14	UDP-glucose:glycoprotein glucosyltransferase 1	sp|Q6P5E4|UGGG1_MOUSE	0	5	0	0.028409	0	0.00012557	5
15	Prolyl 4-hydroxylase subunit alpha-1	sp|Q60715|P4HA1_MOUSE	0	5	0	0.081967	0	0.00036231	5
16	Epoxide hydrolase 1	sp|Q9D379|HYEP_MOUSE	0	9	0	0.169811	0	0.0007506	9
17	Calreticulin	sp|P14211|CALR_MOUSE	0	14	0	0.291667	0	0.00128922	14
18	Sarcoplasmic/endoplasmic reticulum calcium ATPase	sp|O55143|AT2A2_MOUSE	8	18	0.06956522	0.156522	0.0003684	0.00069185	1.8782025
19	Protein disulfide-isomerase A4	sp|P08003|PDIA4_MOUSE	0	12	0	0.166667	0	0.0007367	12
20	Protein disulfide-isomerase	sp|P09103|PDIA1_MOUSE	0	12	0	0.210526	0	0.00093056	12
21	Protein disulfide-isomerase A3	sp|P27773|PDIA3_MOUSE	0	9	0	0.157895	0	0.00069792	9
22	Protein disulfide-isomerase A6	sp|Q922R8|PDIA6_MOUSE	0	11	0	0.229167	0	0.00101296	11
Melanosomes and vesicles membranes									
1	Peptidyl-prolyl cis-trans isomerase B	sp|P24369|PPIB_MOUSE	0	7	0	0.291667	0	0.00128922	7
Cell membrane									
1	T-complex protein 1 subunit gamma	sp|P80318|TCPG_MOUSE	0	2	0	0.032787	0	0.00014492	2
2	Monocarboxylate transporter 4	sp|P57787|MOT4_MOUSE	0	2	0	0.04	0	0.00017681	2
3	Nicastrin	sp|P57716|NICA_MOUSE	0	2	0	0.025641	0	0.00011334	2
4	Basigin	sp|P18572|BASI_MOUSE	0	2	0	0.047619	0	0.00021048	2
5	Vesicle-associated membrane protein-associated protein A	sp|Q9WV55|VAPA_MOUSE	0	3	0	0.107143	0	0.00047359	3
6	Retrovirus-related Env polyprotein from Fv-4	sp|P11370|ENV2_MOUSE	0	3	0	0.040541	0	0.0001792	3
7	Synaptic vesicle membrane protein	sp|Q62465|VAT1_MOUSE	0	4	0	0.093023	0	0.00041118	4
8	4F2 cell-surface antigen heavy chain	sp|P10852|4F2_MOUSE	0	4	0	0.068966	0	0.00030484	4
9	Alpha-enolase	sp|P17182|ENOA_MOUSE	0	5	0	0.106383	0	0.00047023	5
10	Integrin-linked protein kinase	sp|O55222|ILK_MOUSE	0	4	0	0.078431	0	0.00034668	4
11	Transmembrane glycoprotein NMB	sp|Q99P91|GPNMB_MOUSE	2	15	0.03125	0.234375	0.0001655	0.00103598	6.2606749
12	MLV-related proviral Env polyprotein	sp|P10404|ENV1_MOUSE	0	13	0	0.185714	0	0.00082089	13
13	ERO1-like protein alpha	sp|Q8R180|ERO1A_MOUSE	0	5	0	0.092593	0	0.00040928	5
14	Clathrin heavy chain 1	sp|Q68FD5|CLH_MOUSE	0	5	0	0.026042	0	0.00011511	5
15	Desmoglein-1-alpha	sp|Q61495|DSG1A_MOUSE	2	5	0.0173913	0.043478	9.209E-05	0.00019218	2.0868916
16	Sodium/potassium-transporting ATPase subunit alpha-1	sp|Q8VDN2|AT1A1_MOUSE	4	12	0.03539823	0.106195	0.0001874	0.0004694	2.50427

b. Proteins equally enriched by synIgG and alloIgG

	Identified Proteins	Accession Number	C57 SpC	129 SpC	C57 SAF	129 SAF	C57 NSAF	129 NSAF	C57/129 ratio
Endoplasmic reticulum membrane									
1	DnaJ homolog subfamily B member 11	sp|Q99KV1|DJB11_MOUSE	8	6	0.19512195	0.146341	0.0010332	0.00064686	0.6260675
2	78 kDa glucose-regulated protein	sp|P20029|GRP78_MOUSE	73	71	1.01388889	0.986111	0.0053687	0.00435879	0.8118866
3	Serpin H1	sp|P19324|SERPH_MOUSE	11	17	0.23404255	0.361702	0.0012393	0.00159879	1.2900785
4	Protein transport protein Sec61 subunit beta	sp|Q9CQS8|SC61B_MOUSE	2	3	0.2	0.3	0.001059	0.00132605	1.252135
5	Leucine-rich repeat-containing protein 59	sp|Q922Q8|LRC59_MOUSE	3	2	0.08571429	0.057143	0.0004539	0.00025258	0.5565044
6	Protein transport protein Sec61 subunit alpha isoform 1	sp|P61620|S61A1_MOUSE	9	10	0.17307692	0.192308	0.0009165	0.00085003	0.9275074
7	Dolichyl-diphosphooligosaccharide--protein glycosyltransferase 48 kDa subunit	sp|O54734|OST48_MOUSE	3	5	0.06122449	0.102041	0.0003242	0.00045104	1.3912611
8	Estradiol 17-beta-dehydrogenase 12	sp|O70503|DHB12_MOUSE	7	6	0.2	0.171429	0.001059	0.00075774	0.7155057
Melanosomes and vesicles membranes									
1	Flotillin-2	sp|Q60634|FLOT2_MOUSE	3	2	0.06382979	0.042553	0.000338	0.00018809	0.5565044
2	Cathepsin D	sp|P18242|CATD_MOUSE	3	5	0.06666667	0.111111	0.000353	0.00049113	1.3912611
3	AP-2 complex subunit beta	sp|Q9DBG3|AP2B1_MOUSE	8	5	0.07619048	0.047619	0.0004034	0.00021048	0.5217229
4	AP-2 complex subunit mu	sp|P84091|AP2M1_MOUSE	4	5	0.08	0.1	0.0004236	0.00044202	1.0434458
5	Annexin A2	sp|P07356|ANXA2_MOUSE	4	6	0.1025641	0.153846	0.0005431	0.00068003	1.252135
6	Melanocyte protein PMEL	sp|Q60696|PMEL_MOUSE	5	4	0.07575758	0.060606	0.0004011	0.00026789	0.6678053
Cell membrane									
1	Desmoplakin	sp|E9Q557|DESP_MOUSE	63	60	0.18918919	0.18018	0.0010018	0.00079643	0.7950063
2	PDZ domain	sp|Q9Z0G0|GIPC1_MOUSE	13	9	0.36111111	0.25	0.0019121	0.00110504	0.5779085
3	Junction plakoglobin	sp|Q02257|PLAK_MOUSE	37	49	0.45121951	0.597561	0.0023893	0.00264133	1.1054885

c. Proteins enriched by synIgG

	Identified Proteins	Accession Number	C57 SpC	129 SpC	C57 SAF	129 SAF	C57 NSAF	129 NSAF	C57/129 ratio
Endoplasmic reticulum membrane									
1	Stromal cell-derived factor 2-like protein 1	sp|Q9ESP1|SDF2L_MOUSE	3	0	0.125	0	0.0006619	0	3
2	Nicalin	sp|Q8VCM8|NCLN_MOUSE	2	0	0.03174603	0	0.0001681	0	2
3	Translocation protein SEC62	sp|Q8BU14|SEC62_MOUSE	4	0	0.08695652	0	0.0004604	0	4
4	Disco-interacting protein 2 homolog B	sp|Q3UH60|DIP2B_MOUSE	4	0	0.02339181	0	0.0001239	0	4
melanosomes and Vesicles membranes									
1	Vacuolar protein sorting-associated protein 35	sp|Q9EQH3|VPS35_MOUSE	2	0	0.02173913	0	0.0001151	0	2
2	Angiomotin-like protein 2	sp|Q8K371|AMOL2_MOUSE	6	0	0.07058824	0	0.0003738	0	6
3	Fibrous sheath-interacting protein 2	sp|A2ARZ3|FSIP2_MOUSE	9	0	0.01146497	0	6.071E-05	0	9
Cell membrane									

a–**c**, 20 μg of native cell membrane proteins were incubated with 50 μg of syngeneic (C57BL/6) or allogeneic (129S1) IgG coupled to protein G magnetic beads, and precipitated proteins were analysed by mass spectrometry. Shown are conversion to spectral abundance factor (SAF) and subsequent normalized spectral abundance factor (NSAF). This was based on the equation NSAF = (SpC/MW)/Σ(SpC/MW)n; where SpC is spectral counts, MW is protein molecular mass in kDa and n is the total number of proteins.